

# Understanding Self-Distillation and Partial Label Learning in Multi-Class Classification with Label Noise

Hyeonsu Jeong\*

Hye Won Chung†

## Abstract

Self-distillation (SD) is the process of training a student model using the outputs of a teacher model, with both models sharing the same architecture. Our study theoretically examines SD in multi-class classification with cross-entropy loss, exploring both multi-round SD and SD with refined teacher outputs, inspired by partial label learning (PLL). By deriving a closed-form solution for the student model’s outputs, we discover that SD essentially functions as label averaging among instances with high feature correlations. Initially beneficial, this averaging helps the model focus on feature clusters correlated with a given instance for predicting the label. However, it leads to diminishing performance with increasing distillation rounds. Additionally, we demonstrate SD’s effectiveness in label noise scenarios and identify the label corruption condition and minimum number of distillation rounds needed to achieve 100% classification accuracy. Our study also reveals that one-step distillation with refined teacher outputs surpasses the efficacy of multi-step SD using the teacher’s direct output in high noise rate regimes.

## 1 Introduction

Knowledge distillation, initially presented in Hinton et al. (2015), is a technique in machine learning where a smaller, more efficient model (the student) is trained to replicate the behavior and predictions of a larger, complex model (the teacher). The student model achieves this by being trained using the teacher model’s output probability distribution, often in the form of soft labels. This method is typically described as a teacher-student dynamic, where the teacher model delivers “dark knowledge” to the student via these soft labels Chen et al. (2021); Miles et al. (2021); Zhao et al. (2022); Wang et al. (2023b). Knowledge distillation (KD) has been successfully applied in diverse areas such as vision, speech and natural language processing Chebotar & Waters (2016); Cui et al. (2017); Asif et al. (2019); Liu et al. (2019).

The specific scenario in knowledge distillation where both the teacher and student networks share the same architecture is known as *self-distillation* (SD). Surprisingly, SD has also been observed to enhance performance Furlanello et al. (2018); Zhang et al. (2019). This phenomenon cannot be easily explained by the conventional theory that attributes KD’s improvements to the student mimicking a more complex teacher with higher capacity. Recent studies have aimed to theoretically analyze the effects of self-distillation in analytically simpler settings. For instance, Mobahi et al. (2020); Dong et al. (2019) explored the advantages of SD in classical regression problems using mean squared error. Phuong & Lampert (2019) considered binary classification with cross-entropy (CE) loss in linear networks, examining how distillation-trained classifiers improve generalization and convergence rates. Das & Sanghavi (2023) investigated SD in the presence of label noise in binary classification with CE loss, identifying the corruption regime where the student outperforms the teacher. However, fully understanding and quantifying the benefits of SD, especially in *multi-class* classification with CE loss—a widely used classification framework—remains a significant, unresolved challenge.

In this work, we theoretically analyze self-distillation (SD) in multi-class classification with CE loss, both for multi-round SD and SD with refined soft labels. We derive closed form solutions for the outputs of the student model as the distillation round increases. The technical challenge in the analysis lies in the

\*School of Electrical Engineering, KAIST, Daejeon, 34141, Korea. email: [hsjeong1121@kaist.ac.kr](mailto:hsjeong1121@kaist.ac.kr)

†School of Electrical Engineering, KAIST, Daejeon, 34141, Korea. email: [hwchung@kaist.ac.kr](mailto:hwchung@kaist.ac.kr)

non-linearity of softmax functions. We tackle this by imposing a linear approximation of softmax (similar to the original paper Hinton et al. (2015)) and justifying it through theoretical analysis and experiments.

Our analysis reveals a novel insight on the effect of self-distillation; self-distillation can be interpreted as label averaging among instances sharing high feature correlations, in predicting the true label for a given instance. Especially, by assuming that the training instances of the same ground-truth class has a higher feature correlation than the instances from different classes, which is a feasible assumption to train a classifier, we show that the (multi-round) self-distillation is equivalent to (repeatedly) multiplying an approximately block-structured transformation matrix to the matrix of given labels (one-hot vectors). The transformation matrix effectively averages the labels of instances having high feature correlations. By analyzing the eigenspectrum of this transformation matrix as the distillation round  $t$  increases, we reveal that a few round of distillation makes the top- $K$  (equal to the number of classes) eigenvalues dominate the rest eigenvalues, helping the student model to focus on the feature clusters in predicting the labels. However, as distillation round continues to increase, only the top-1 eigenvalue dominates the rest, resulting in worse performance.

We further demonstrate that SD is especially beneficial in the presence of label noise, and identify the conditions for label corruption and minimum number of distillation rounds needed to achieve 100% population accuracy. We also explore the advantages of using refined soft labels, inspired by partial label learning (PLL) Cour et al. (2011), which is typically employed in weak supervision tasks where training samples are associated with a set of candidate labels rather than a single ground truth. Our approach utilizes a candidate set of the top-two feasible labels, refined from the teacher’s output. We demonstrate that in high label noise rate, SD with PLL yields greater performance improvements compared to traditional SD methods that directly use the teacher’s output without any refinement. Up to our knowledge, this is the first theoretical work demonstrating the superiority of SD using PLL in high noise rate regime.

We validate our theoretical findings through experimental results on both synthetic and real datasets. These experiments confirm the effectiveness of multi-round SD and SD with PLL, particularly in the presence of label noise.

## 2 Related Work

**Knowledge Distillation** Following its initial introduction Hinton et al. (2015) and various extensions Romero et al. (2014); Tian et al. (2019); Lopez-Paz et al. (2015), a number of studies have attempted to theoretically analyze the effects of knowledge distillation (KD) and self-distillation (SD). Especially, most of papers have imposed particular assumptions on either training dataset, model architecture, and/or loss function for analytically tractable solutions.

Mobahi et al. (2020); Dong et al. (2019) analyzed the benefits of SD in regression problems with mean squared error. Mobahi et al. (2020) focused on fitting a function to training instances with  $\ell_2$  regularization in the function space, and showed that multi-round SD progressively reduces the number of basis, preventing over-fitting for a few rounds, but inducing under-fitting after certain rounds. Dong et al. (2019) also showed that early-stopping is crucial in SD.

There also exist some previous works that analyzed the effect of distillation in *binary* classification with cross-entropy loss. Phuong & Lampert (2019); Ji & Zhu (2020) considered knowledge distillation, in linear networks or in wide neural networks, and analyzed the generalization of the distillation-trained classifiers. Das & Sanghavi (2023) analyzed self-distillation in logistic regression in the presence of label noise. The range of label corruption where student outperforms the teacher was quantified, by approximating a sigmoid function using the first-order Maclaurin series.

In contrast, our paper considers *multi-class classification* with the cross-entropy loss, which is a more general and practical setup for classification. Our analysis reveals that the effect of self-distillation can be interpreted as *label averaging* among the instances sharing high feature correlations. Some previous works also provided diverse interpretations on the effect of self-distillation in multi-class classification. For example, Zhang et al. (2019) related SD to instance-specific label smoothing, which penalizes over-confident predictions and promotes confidence diversity by smoothing out ground-truth labels using the teacher’s softmax outputs.

Allen-Zhu & Li (2022) analyzed the impact of self-distillation, along with ensemble and knowledge distillation in a unified framework, on a *multi-view* dataset.

One of the main distinctions of our work from all these previous works is that we demonstrate the benefits of SD with partial label learning (in addition to multi-round SD), and quantify the range of label corruptions where the student model with PLL outperforms both the multi-round self-distillation and teacher model. This also provides a new way of distilling the “dark knowledge” of the teacher model, not directly using the teacher’s softmax output but by refining the outputs as a candidate set of *feasible* labels.

**Partial label learning** The goal of PLL is to train a classifier with a set of candidate labels on each instance so that it can produce the correct classification with high probability. Many works have elaborately designed learning objectives to achieve this goal, for example by weighting candidates using logits in the training process Lv et al. (2020); Wang et al. (2021) or inferring label distributions using topological information in the feature space Wang et al. (2019); Xu et al. (2019); Lyu et al. (2019). Recently, noisy-PLL, where the candidate set does not contain true labels, has also been addressed Xu et al. (2023); Wang et al. (2023a); Lian et al. (2022). In contrast, assuming that noisy *hard* labels are given to the teacher model, we derive the condition that the teacher’s softmax output always includes the ground-truth label in the top-two labels. Under the condition, we show that the student model can achieve 100% population accuracy by the self-distillation with the refined softmax labels. Our work demonstrates the benefits of SD using PLL over the traditional SD in high noise rate regime.

### 3 Problem Setup

We consider the problem of  $K$ -class classification in which each sample  $\mathbf{x} \in \mathcal{X}$  is associated with the class  $y(\mathbf{x}) \in \mathcal{Y} := \{1, 2, \dots, K\}$ . Let  $\mathcal{P}$  be the underlying distribution over the sample space  $\mathcal{X} \times \mathcal{Y}$ . We assume that a feature map  $\phi : \mathcal{X} \rightarrow \tilde{\mathcal{X}} \subset \mathbb{R}^d$  is given, and a dataset  $\{\phi(\mathbf{x}_i), \hat{y}_i\}_{i=1}^{Kn}$  is composed of feature-label pairs  $(\phi(\mathbf{x}_i), \hat{y}_i) \in \tilde{\mathcal{X}} \times \mathcal{Y}$ . The provided label  $\hat{y}_i$  can be noisy. We denote the true label by  $y_i = y(\mathbf{x}_i)$ . Assume that the dataset is balanced with respect to both the ground-truth labels and provided labels, i.e.,  $|\{i : y_i = k\}| = |\{i : \hat{y}_i = k\}| = n$  for  $\forall k \in [K]$ .

We are interested in finding a classifier for the data with respect to the ground-truth labels by using a multinomial logistic regression (softmax regression). This problem is equivalent to linear probing within a neural network context, where the network is composed of a fixed feature extractor  $\phi : \mathcal{X} \rightarrow \tilde{\mathcal{X}}$  followed by a tunable fully connected linear layer, parameterized by  $\boldsymbol{\theta} \in \mathbb{R}^{d \times K}$ , and a softmax layer:

$$\mathbf{y} = \sigma^\tau(\boldsymbol{\theta}^\top \phi(\mathbf{x})), \quad (1)$$

where the softmax  $\sigma^\tau : \mathbb{R}^K \rightarrow (0, 1)^K$  is defined by

$$\sigma^\tau(\mathbf{v}) = \left[ \frac{\exp(v_1/\tau)}{\sum_{i=1}^K \exp(v_i/\tau)}, \dots, \frac{\exp(v_K/\tau)}{\sum_{i=1}^K \exp(v_i/\tau)} \right] \quad (2)$$

for the logits  $\mathbf{v} \in \mathbb{R}^K$  where  $\tau$  is a temperature. In this work, we set  $\tau = 1$  and denote  $\sigma^1(\cdot) = \sigma(\cdot)$ . In Appendix D.1, we show that the temperature scaling of the softmax, combined with the proper scaling of the cross-entropy (CE) loss function in the regularized CE loss (3), results in the same optimal solution for  $\boldsymbol{\theta}$  as in  $\tau = 1$ . The class prediction by the model is given by  $\arg \max_{k \in [K]} [\sigma(\boldsymbol{\theta}^\top \phi(\mathbf{x}))]_k$ . We are interested in the population accuracy of the model:  $\mathbb{E}_{(\mathbf{x}, y(\mathbf{x})) \sim \mathcal{P}} \left[ \mathbb{1} \left( \arg \max_{k \in [K]} [\sigma(\boldsymbol{\theta}^\top \phi(\mathbf{x}))]_k = y(\mathbf{x}) \right) \right]$ . The same classifier architecture, parameterized by  $\boldsymbol{\theta} \in \mathbb{R}^{d \times K}$ , is used both for the teacher and the student. We aim to find a condition where the student model achieves better classification accuracy than the teacher model.

**Teacher Model** The teacher’s objective is to minimize the  $\ell_2$ -regularized cross-entropy loss between the given labels and its predictions:

$$f_T(\boldsymbol{\theta}) = \frac{1}{Kn} \sum_{i=1}^{Kn} \text{CE}(\mathbf{e}(\hat{y}_i), \mathbf{y}_i^{(T)}) + \frac{\lambda \|\boldsymbol{\theta}\|_F^2}{2}, \quad (3)$$

where  $\mathbf{e}(i)$  is the one-hot encoded vector of label  $i \in [K]$ , having 1 in the  $i$ -th entry and 0 for the rest, and  $\mathbf{y}_i^{(T)} = \sigma(\boldsymbol{\theta}^\top \phi(\mathbf{x}_i))$  is the output of the model for input  $\mathbf{x}_i$ . The cross-entropy loss is defined by  $\text{CE}(\mathbf{e}(\hat{y}_i), \mathbf{y}_i^{(T)}) := -\sum_{k=1}^K [\mathbf{e}(\hat{y}_i)]_k \log[\mathbf{y}_i^{(T)}]_k$ . Denote the teacher’s optimal parameter  $\boldsymbol{\theta}$  by  $\boldsymbol{\theta}_T := \arg \min_{\boldsymbol{\theta}} f_T(\boldsymbol{\theta})$ . Then, the optimal  $\boldsymbol{\theta}_T$  making  $\frac{df_T(\boldsymbol{\theta})}{d\boldsymbol{\theta}} = 0$  is

$$\boldsymbol{\theta}_T^\top = \sum_{i=1}^{Kn} \underbrace{\frac{1}{Kn\lambda} (\mathbf{e}(\hat{y}_i) - \mathbf{y}_i^{(T)})}_{:=\boldsymbol{\alpha}_i} \phi(\mathbf{x}_i)^\top = \sum_{i=1}^{Kn} \boldsymbol{\alpha}_i \phi(\mathbf{x}_i)^\top. \quad (4)$$

**Student Model with Multi-Round Self-Distillation** In self-distillation, the student model has the same architecture as the teacher model, but the model targets the teacher’s output  $\mathbf{y}_i^{(T)}$  instead of the given labels in minimizing the regularized cross-entropy loss. Self-distillation can be repeated iteratively such that the  $t$ -th distilled model uses the output of the  $(t-1)$ -th distilled model as targets in the training objective. When  $\mathbf{y}_i^{(t-1)}$  denotes the output of the  $(t-1)$ -th distilled model for the  $i$ -th sample, the training objective for the  $t$ -th distilled model is given by

$$f^{(t)}(\boldsymbol{\theta}) = \frac{1}{Kn} \sum_{i=1}^{Kn} \text{CE}(\mathbf{y}_i^{(t-1)}, \mathbf{y}_i^{(t)}) + \frac{\lambda \|\boldsymbol{\theta}\|_F^2}{2}, \quad (5)$$

where  $\mathbf{y}_i^{(t)} = \sigma(\boldsymbol{\theta}^\top \phi(\mathbf{x}))$  for  $t \in \mathbb{Z}^+$ . Note that  $f^{(1)}(\boldsymbol{\theta})$  is the objective of the teacher model (3) where  $\mathbf{y}_i^{(0)} := \mathbf{e}(\hat{y}_i)$ . Then, the optimal  $\boldsymbol{\theta}$  of the  $t$ -th distilled model, denoted by  $\boldsymbol{\theta}^{(t)}$ , is given by

$$\boldsymbol{\theta}^{(t)\top} = \sum_{i=1}^{Kn} \underbrace{\frac{1}{Kn\lambda} (\mathbf{y}_i^{(t-1)} - \mathbf{y}_i^{(t)})}_{:=\boldsymbol{\alpha}_i^{(t)}} \phi(\mathbf{x}_i)^\top = \sum_{i=1}^{Kn} \boldsymbol{\alpha}_i^{(t)} \phi(\mathbf{x}_i)^\top. \quad (6)$$

**Student Model with Partial Label Learning** Partial label learning (PLL) trains a classifier by using the candidate set of labels for each input instance Cour et al. (2011). Following PLL, we also consider a student model not directly targeting the output of the teacher model but the candidate set of labels selected from the teacher output. In particular, we consider generating a two-hot vector  $\bar{\mathbf{y}}_i$  from the teacher output  $\mathbf{y}_i^{(T)}$  by selecting the top two labels of the highest values and putting 1/2 on those labels while zeroing out other values. The objective for the student model with PLL is then defined as follows:

$$f_P(\boldsymbol{\theta}) = \frac{1}{Kn} \sum_{i=1}^{Kn} \text{CE}(\bar{\mathbf{y}}_i, \mathbf{y}_i^{(P)}) + \frac{\lambda \|\boldsymbol{\theta}\|_F^2}{2}, \quad (7)$$

where  $\mathbf{y}_i^{(P)} = \sigma(\boldsymbol{\theta}^\top \phi(\mathbf{x}))$ . When  $\boldsymbol{\theta}_P$  denotes the optimal parameter minimizing  $f_P(\boldsymbol{\theta})$ , it satisfies

$$\boldsymbol{\theta}_P^\top = \sum_{i=1}^{Kn} \underbrace{\frac{1}{Kn\lambda} (\bar{\mathbf{y}}_i - \mathbf{y}_i^{(P)})}_{:=\boldsymbol{\gamma}_i} \phi(\mathbf{x}_i)^\top = \sum_{i=1}^{Kn} \boldsymbol{\gamma}_i \phi(\mathbf{x}_i)^\top. \quad (8)$$

**Two Assumptions for Analytical Solution** Since the teacher and the student use the same architecture as well as the loss function, except for their targets, the optimal solutions have the same form as in (4), (6) and (8), a linear combination of input features  $\{\phi(\mathbf{x}_i)\}$  with the sample-dependent coefficients. We impose an assumption on the feature map  $\phi(\cdot)$  to compare these solutions analytically.

**Assumption 1.** (Feature correlation in the training set) The features have unit norm  $\|\phi(\mathbf{x})\|_2 = 1, \forall \mathbf{x} \in \mathcal{X}$ , and the inner product between two features  $\langle \phi(\mathbf{x}_i), \phi(\mathbf{x}_j) \rangle$  is a function of the corresponding true labels  $y_i$  and  $y_j$ , i.e.,

$$\langle \phi(\mathbf{x}_i), \phi(\mathbf{x}_j) \rangle = \omega(y_i, y_j) \text{ for } i \neq j. \quad (9)$$

This assumption can be relaxed to  $\mathbb{E}[\langle \phi(\mathbf{x}_i), \phi(\mathbf{x}_j) \rangle] = \omega(y_i, y_j)$  when we have enough number  $n$  of samples. In Appendix A.1, we empirically demonstrate the feasibility of the assumption on a real dataset, CIFAR-100.

By Assumption 1, for  $\boldsymbol{\theta}_T^\top$  in (4), we have  $\boldsymbol{\theta}_T^\top \phi(\mathbf{x}_i) = \sum_{j=1}^{Kn} \boldsymbol{\alpha}_j \phi(\mathbf{x}_j)^\top \phi(\mathbf{x}_i) = (1 - \omega(y_i, y_i)) \boldsymbol{\alpha}_i + \mathbf{s}_\alpha(y_i)$  where  $\mathbf{s}_\alpha(y_i) := \sum_{j=1}^{Kn} \omega(y_i, y_j) \boldsymbol{\alpha}_j$ . Thus,  $\boldsymbol{\alpha}_i$  in (4) satisfies

$$Kn\lambda \boldsymbol{\alpha}_i = \mathbf{e}(\hat{y}_i) - \sigma((1 - \omega(y_i, y_i)) \boldsymbol{\alpha}_i + \mathbf{s}_\alpha(y_i)). \quad (10)$$

Similar equations can be obtained for the coefficients  $\boldsymbol{\alpha}_i^{(t)}$  and  $\gamma_i$  of the student models in (6) and (8) by replacing  $\mathbf{e}(\hat{y}_i)$  in (10) with the students' new targets,  $\mathbf{y}_i^{(t-1)}$  and  $\bar{\mathbf{y}}_i$ , respectively. In solving (10) for  $\boldsymbol{\alpha}_i$ , the main challenge comes from non-linearity of the softmax function. To resolve this, we approximate the softmax as follows:

**Assumption 2** (Linear approximation of softmax). We approximate the softmax  $\sigma(\mathbf{v})$  by

$$\begin{aligned} \sigma(\mathbf{v}) &= \left[ \frac{\exp(v_1)}{\sum_{i=1}^K \exp(v_i)}, \dots, \frac{\exp(v_K)}{\sum_{i=1}^K \exp(v_i)} \right] \\ &\approx \left[ \frac{1 + v_1}{K + \sum_{i=1}^K v_i}, \dots, \frac{1 + v_K}{K + \sum_{i=1}^K v_i} \right]. \end{aligned} \quad (11)$$

This type of linear approximation was considered in analyzing the effect of knowledge distillation in Hinton et al. (2015), where the softmax output layer converts the logits  $\mathbf{v}$  by  $\sigma(\mathbf{v}/\tau)$  with a high temperature  $\tau > 0$ . When we set  $\tau = 1$ , the approximation is still valid if the logits have small enough magnitudes. From (6), the logits of the  $t$ -th distilled model for input  $\phi(\mathbf{x}_i)$  is given by  $\boldsymbol{\theta}^{(t)\top} \phi(\mathbf{x}_i) = \sum_{j=1}^{Kn} \phi(\mathbf{x}_j)^\top \phi(\mathbf{x}_i) \boldsymbol{\alpha}_j^{(t)}$ , equivalent to

$$\sum_{j=1}^{Kn} \frac{\phi(\mathbf{x}_j)^\top \phi(\mathbf{x}_i)}{Kn\lambda} \left( \sigma(\boldsymbol{\theta}^{(t-1)} \phi(\mathbf{x}_j)) - \sigma(\boldsymbol{\theta}^{(t)} \phi(\mathbf{x}_j)) \right).$$

Thus, the magnitude of logits becomes small if the *averaged* difference between the softmax outputs of the teacher (here, the  $(t-1)$ -th distilled model) and the student model ( $t$ -th distilled model) over all training instances is small enough. In Fig. 1 and Appx. A.2, we empirically demonstrate that this condition is well satisfied for the class-balanced datasets. Assuming logits are zero-means, i.e.,  $\sum_{i=1}^K v_i = 0$ , which always holds in our model since  $\mathbf{v} = \boldsymbol{\theta}_T^\top \phi(\mathbf{x}_i) = \sum_{j=1}^{Kn} \boldsymbol{\alpha}_j \phi(\mathbf{x}_j)^\top \phi(\mathbf{x}_i)$  and  $\sum_{k=1}^K [\boldsymbol{\alpha}_j]_k = 0$  for all  $j$ , we have

$$\sigma(\mathbf{v}) \approx \sigma_L(\mathbf{v}) := \frac{1}{K} \mathbf{1}_K + \frac{1}{K} \mathbf{v} \quad (12)$$

where  $\mathbf{1}_K$  refers to the vector of all 1's with length  $K$ . The softmax output is thus approximated to a uniform vector  $\mathbf{1}_K/K$  perturbed by a (scaled) logit  $\mathbf{v}$ .

Our analysis in Sec. 4 will be based on Assumptions 1 and 2. We will analytically solve the closed form solutions of the teacher and student models' outputs and identify the conditions for the student to outperform the teacher. In Sec. 5, we will show that our theoretical analysis aligns well with empirical results, showing the benefits of self-distillation and PLL, for the cases where the assumptions are well held.

## 4 Main Results

In this section, we will analyze the effect of multi-round SD and SD using PLL.

### 4.1 Closed Form Solution of Model Outputs

We will provide a closed form solution for the outputs of the teacher and student models for input instances in the training dataset. For the concise presentation, we first introduce some matrix definitions and notations. Let us define matrices  $\mathbf{Y}^{(t)}$ ,  $\mathbf{Y}^{(P)}$ ,  $\mathbf{P} \in \mathbb{R}^{K \times K_n}$  by

$$\begin{aligned} \mathbf{Y}^{(t)} &:= [\mathbf{y}_1^{(t)}, \dots, \mathbf{y}_{K_n}^{(t)}]; & \mathbf{Y}^{(P)} &:= [\mathbf{y}_1^{(P)}, \dots, \mathbf{y}_{K_n}^{(P)}]; \\ \mathbf{P} &:= [\mathbf{e}(y_1), \dots, \mathbf{e}(y_{K_n})], \end{aligned}$$

where  $\mathbf{Y}^{(t)}$  and  $\mathbf{Y}^{(P)}$  denote the outputs of the student models after the  $t$ -th distillation and by PLL, respectively, for inputs of the training dataset  $\{\phi(\mathbf{x}_i), \hat{y}_i\}_{i=1}^{K_n}$ .  $\mathbf{P}$  is the matrix of ground-truth labels for  $\{\phi(\mathbf{x}_i)\}_{i=1}^{K_n}$ .

We also define a symmetric matrix  $\mathbf{W} \in \mathbb{R}^{K \times K}$  by

$$[\mathbf{W}]_{x,y} := \frac{\omega(x,y)}{K^2 n \lambda + 1 - \omega(x,x)}, \quad (13)$$

for  $x, y \in [K]$  using the feature correlation  $\omega(x, y)$  in (9), and define a vector  $\mathbf{v} \in \mathbb{R}^K$  by  $\mathbf{v} := [c(1), \dots, c(K)]$  where  $c(y) := \frac{K n \lambda}{K^2 n \lambda + 1 - \omega(y,y)}$  for  $y \in [K]$ . Let  $\mathbf{D}(\mathbf{x}) \in \mathbb{R}^{K \times K}$  denote a diagonal matrix with its diagonal entries equal to  $\mathbf{x} \in \mathbb{R}^K$ . Lastly, we define

$$\mathbf{B} := \mathbf{D}(\mathbf{v}\mathbf{P}) - \mathbf{P}^\top \mathbf{W}^\top (\mathbf{I}_K + n\mathbf{W}^\top)^{-1} \mathbf{D}(\mathbf{v})\mathbf{P}. \quad (14)$$

We present the closed form solutions for the outputs of the student models in terms of  $\mathbf{B}$ .

**Lemma 1.** *The output  $\mathbf{Y}^{(t)} \in \mathbb{R}^{K \times K_n}$  of the  $t$ -th distilled model for inputs of the training dataset  $\{\phi(\mathbf{x}_i), \hat{y}_i\}_{i=1}^{K_n}$  is given by*

$$\mathbf{Y}^{(t)} = \left( \mathbf{Y}^{(0)} - \frac{1}{K} \mathbf{1}_{K \times K_n} \right) (\mathbf{I}_{K_n} - K\mathbf{B})^t + \frac{1}{K} \mathbf{1}_{K \times K_n}, \quad (15)$$

and that of the student model trained by PLL is given by

$$\mathbf{Y}^{(P)} = \left( \bar{\mathbf{Y}} - \frac{1}{K} \mathbf{1}_{K \times K_n} \right) (\mathbf{I}_{K_n} - K\mathbf{B}) + \frac{1}{K} \mathbf{1}_{K \times K_n}, \quad (16)$$

for  $\mathbf{Y}^{(0)} := [\mathbf{e}(\hat{y}_1), \dots, \mathbf{e}(\hat{y}_{K_n})]$  and  $\bar{\mathbf{Y}} = [\bar{y}_1, \dots, \bar{y}_{K_n}]$ .

**Remark 1** (Effect of self-distillation). As shown by (15), the self-distillation effectively multiplies the given label matrix  $(\mathbf{Y}^{(0)} - \frac{1}{K} \mathbf{1}_{K \times K_n})$  by the  $t$ -th power of  $(\mathbf{I}_{K_n} - K\mathbf{B})$  as it iterates  $t$  rounds. The matrix  $(\mathbf{I}_{K_n} - K\mathbf{B})$  depends on the ground-truth labels  $\mathbf{P}$  and the feature correlations between classes, represented by  $\mathbf{W}$  and  $\mathbf{v}$ . The characteristics of  $(\mathbf{I}_{K_n} - K\mathbf{B})$ , especially the eigenvectors and eigenvalues (if diagonalizable), reveal the *clusterability* of input instances into the correct  $K$ -classes solely using their input correlations. Multiplying  $(\mathbf{I}_{K_n} - K\mathbf{B})^t$  to  $(\mathbf{Y}^{(0)} - \frac{1}{K} \mathbf{1}_{K \times K_n})$  in generating the model outputs leads to making decisions on each input instance not merely relying on the provided label  $\mathbf{e}(\hat{y})$  but by exploiting the labels of instances having feature correlations with the given input instance. When we denote the eigenvalues of  $(\mathbf{I}_{K_n} - K\mathbf{B})$  by  $\lambda_1 \geq \dots \geq \lambda_{K_n} \geq 0$ , the eigenvalues of  $(\mathbf{I}_{K_n} - K\mathbf{B})^t$  becomes  $\lambda_1^t \geq \dots \geq \lambda_{K_n}^t \geq 0$ . As  $t$  increases, the gap between the top- $K$  eigenvalues and the rest, or  $|\lambda_K^t - \lambda_{K+1}^t|$ , increases, making the distilled model more focus on the major top- $K$  eigenvectors in label averaging. This can help improving the classification accuracy of the distilled model, especially when the given labels are noisy as will be shown in Theorem 1, since the

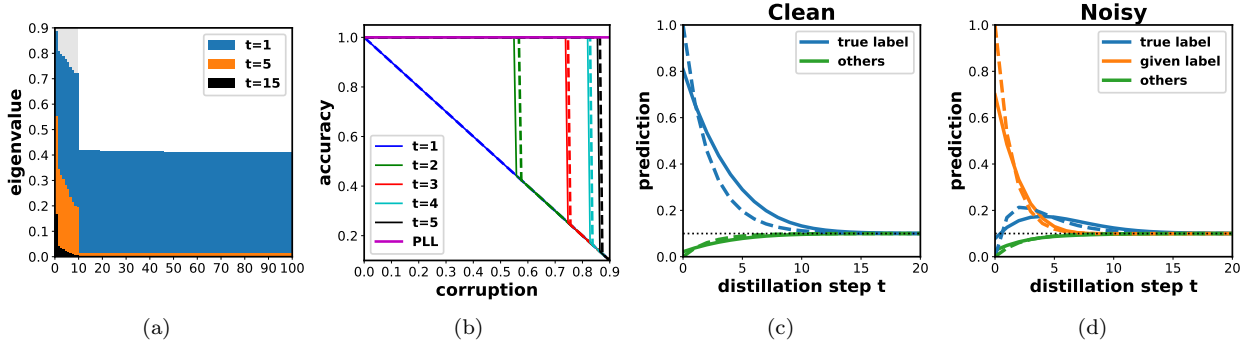


Figure 1: (a) The evolution of the eigenvalues of  $(\mathbf{I}_{K^n} - K\mathbf{B})^t$  as the number  $t$  of distillation rounds increases, for a feature correlation  $\omega(\cdot, \cdot)$ , randomly sampled while ensuring  $\omega(y_i, y_i) > \omega(y_i, y_j)$  for  $K = 10$  class. Initially, only the top 10 eigenvalues—corresponding to the eigenvectors of the ground-truth block structure  $\mathbf{P}^\top \mathbf{P}$ —stand out for the first few rounds (e.g., at  $t = 5$ ). However, with an increase in the number of rounds (e.g., at  $t = 15$ ), the top-1 eigenvalue becomes increasingly dominant, while the remaining eigenvalues converge towards zero. (b) The accuracy of the models as the label corruption rate increases for different number  $t$  of distillation rounds and PLL. The solid lines are the results obtained by numerically solving (10) without applying Assm. 2 (linearization of softmax), while the dotted lines are the results from Thm. 1. The 100% population accuracy regime increases as the distillation round  $t$  increase, and PLL maintains 100% population accuracy up to the 90% corruption. We use  $K = 10$ ,  $n = 100$ ,  $\lambda = 10^{-4}$ ,  $c = 0.02$  and  $d = 0.01$ , assuming the feature correlation (17). (c) and (d) represent the changes in output prediction for both clean and noisy samples as the distillation round  $t$  increases. For clean samples, the true label prediction maintains the highest value, while for noisy samples, the true label prediction starts lower than the given label but surpasses it in the first few rounds. As  $t$  increases further, all predictions become uniform.

model prediction incorporates the (approximately) *rank- $K$  block structure* of  $(\mathbf{I}_{K^n} - K\mathbf{B})^t$ , inferred from the input correlations, for label averaging. However, as  $t$  increases further, only the top-1 eigenvector dominates the decision since  $\lambda_1^t \gg \lambda_2^t$  as  $t \rightarrow \infty$  (if  $\lambda_1 > \lambda_2$ ), resulting in meaningless decision for  $K$ -class classification. For the output of PLL (16), on the other hand, the self-distillation effect is reflected by the refined two-hot labels  $\bar{\mathbf{Y}}$  for input instances, obtained from the teacher output. If the teacher’s softmax output contains the ground-truth label in the highest top two values more frequently than any other incorrect labels on average, using  $\bar{\mathbf{Y}}$  instead of the given labels  $\mathbf{Y}^{(0)}$  helps improving the classification accuracy, as will be demonstrated in Theorem 2.

To provide more concrete discussions on the effect of self-distillation, we consider a particular class-wise feature correlation pattern such that:

$$\langle \phi(\mathbf{x}_i), \phi(\mathbf{x}_j) \rangle = \omega(y_i, y_j) = \begin{cases} c, & y_i = y_j, \\ d, & y_i \neq y_j, \end{cases} \quad (17)$$

for some  $c > d > 0$ . This feature correlation makes the matrix  $\mathbf{B}$  in (14) symmetric and thus diagonalizable, and  $(\mathbf{I}_{K^n} - K\mathbf{B})^t$  in (15) can be simplified as

$$(\mathbf{I}_{K^n} - K\mathbf{B})^t = p^t \mathbf{I}_{K^n} + \frac{q^t - p^t}{n} \mathbf{P}^\top \mathbf{P} + \frac{r^t - q^t}{Kn} \mathbf{1}_{K^n \times K^n} \quad (18)$$

where

$$\begin{aligned} p &:= 1 - (K^2 n \lambda) / (K^2 n \lambda + 1 - c), \\ q &:= 1 - (K^2 n \lambda) / (K^2 n \lambda + 1 - c + n(c - d)), \\ r &:= 1 - (K^2 n \lambda) / (K^2 n \lambda + 1 - c + n(c - d) + Knd). \end{aligned} \quad (19)$$

Note that  $0 \leq p \leq q \leq r \leq 1$  where  $p = q$  if  $c = d$  and  $q = r$  if  $d = 0$ . Using the assumption that the dataset is balanced with respect to the ground-truth labels and further assuming (*w.l.o.g.*) that the training instances are ordered based on their ground-truth labels, we get a block diagonal matrix for  $\mathbf{P}^\top \mathbf{P} \in \mathbb{R}^{Kn \times Kn}$  in (18), which is a square matrix such that the main-diagonal blocks are all-1  $n \times n$  square matrices and all off-diagonal blocks are zero matrices.  $[\mathbf{P}^\top \mathbf{P}]_{i,j}$  indicates whether the  $i$ -th and  $j$ -th instances share the same ground-truth labels ( $[\mathbf{P}^\top \mathbf{P}]_{i,j} = 1$ ) or not ( $[\mathbf{P}^\top \mathbf{P}]_{i,j} = 0$ ). Thus, multiplying  $\mathbf{Y}^{(0)}$  by  $\mathbf{P}^\top \mathbf{P}$  results in label averaging among the instances having the same ground-truth labels. For better classification accuracy, the signal from  $\mathbf{Y}^{(0)} \mathbf{P}^\top \mathbf{P}$  should be larger than those from  $\mathbf{Y}^{(0)} \mathbf{I}_{Kn}$ , the outputs depending only on the given (noisy) labels, or from  $\mathbf{Y}^{(0)} \mathbf{1}_{Kn \times Kn}$ , the mere averaging of labels over *all* training instances. The weights on three terms in (18) change depending on the distillation round  $t$ , and those weights determine the eigenvalues of  $(\mathbf{I}_{Kn} - K\mathbf{B})^t$ :

$$(r^t, \underbrace{q^t, \dots, q^t}_{K-1}, \underbrace{p^t, \dots, p^t}_{Kn-K}). \quad (20)$$

The first  $K$  eigenvalues are associated with the eigenvectors of  $\mathbf{P}^\top \mathbf{P}$ , containing the information for clustering, while the rest  $(Kn - K)$  eigenvalues and the corresponding eigenvectors do not include any information for clustering. For  $c > d > 0$ , we have  $r > q > p$  from the definition (19). Thus, for a few rounds, the top  $K$  eigenvalues dominate the rest of  $(Kn - K)$  eigenvalues, i.e., the gap  $(q^t - p^t)$  increases, resulting in better classification performance. However, as  $t$  increases further, only the top-1 eigenvalue (with all-1 eigenvector) dominates the rest of the eigenvectors, resulting in making output for every instance by merely averaging out the labels of the entire training instances. An example of eigenspectrum of  $(\mathbf{I}_{Kn} - K\mathbf{B})^t$  as the distillation round  $t$  increases is illustrated in Fig.1a.

By using (18) and Lemma 1, with the assumption that the dataset is balanced with respect to the provided labels, the outputs of the student models can be simplified as follows.

**Lemma 2.** *Assuming the feature correlation (17), the output of the  $t$ -th distilled model for input  $\phi(\mathbf{x}_i)$  of the training dataset  $\{\phi(\mathbf{x}_i), \hat{y}_i\}_{i=1}^{Kn}$  is given by*

$$\mathbf{y}_i^{(t)} = p^t \mathbf{e}(\hat{y}_i) + (q^t - p^t) \left( \frac{1}{n} \sum_{\{j: y_i = y_j\}} \mathbf{e}(\hat{y}_j) \right) + \frac{(1 - q^t)}{K} \mathbf{1}_K \quad (21)$$

and that by PLL is given by

$$\mathbf{y}_i^{(P)} = p \bar{\mathbf{y}}_i + (q - p) \left( \frac{1}{n} \sum_{\{j: y_i = y_j\}} \bar{\mathbf{y}}_j \right) + \frac{(1 - q)}{K} \mathbf{1}_K. \quad (22)$$

Note that the  $\mathbf{y}_i^{(t)}$  in (21) is a linear combination of 1) the provided label  $\mathbf{e}(\hat{y}_i)$ , 2) the average of label vectors among the instances of the same ground-truth label as  $\mathbf{x}_i$ ,  $\frac{1}{n} \sum_{\{j: y_i = y_j\}} \mathbf{e}(\hat{y}_j)$ , and 3) the uniform vector  $\frac{1}{K} \mathbf{1}_K$ . The weights on each term are  $p^t$ ,  $(q^t - p^t)$  and  $(1 - q^t)$ , respectively. Since  $1 > q > p > 0$ , as the distillation round  $t$  increases, the output becomes less dependent on the provided label but more on the average label vector of the samples of the same ground-truth class. As  $t$  increases further, the output converges to the uniform vector since  $p^t, q^t \rightarrow 0$  as  $t \rightarrow \infty$ . The proof of Lemma 2 and analysis for other types of feature correlations are available in Appendix E.

## 4.2 Self-Distillation as Prediction Averaging

In this section, we compare the performances of the teacher and the student models with multi-round self-distillation and identify the condition for the student model to outperform the teacher model. For the analysis, we use Lemma 2, assuming the feature correlation (17). The performance of each model  $\theta$  is measured by the population accuracy,  $\mathbb{E}_{(\mathbf{x}, y(\mathbf{x})) \sim \mathcal{P}} \left[ \mathbb{1} \left( \arg \max_{k \in [K]} [\sigma(\theta^\top \phi(\mathbf{x}))]_k = y(\mathbf{x}) \right) \right]$ .

Let us define the label corruption matrix  $\mathbf{C} \in \mathbb{R}^{K \times K}$  by

$$[\mathbf{C}]_{k,k'} := |\{i : y_i = k, \hat{y}_i = k'\}| / n. \quad (23)$$



In the theorem below, we state the condition for the student model to outperform the teacher model in terms of the class-wise label corruption rate  $\mathbf{C}$  and the parameters  $p, q$  in (19).

**Theorem 1.** *Suppose that we have access to the population, i.e.,  $n \rightarrow \infty$ . Under Assumptions 1, 2 and (17), the  $t$ -th distilled model achieves 100% population accuracy if*

$$[\mathbf{C}]_{k,k} > [\mathbf{C}]_{k,k'} + \frac{1}{(q/p)^t - 1}, \quad \forall k, k' (\neq k) \in [K]. \quad (24)$$

Furthermore, if (24) holds and there exists  $k, k' \in [K]$ ,  $k \neq k'$ , such that

$$[\mathbf{C}]_{k,k'} + \frac{1}{(q/p)^{t-1} - 1} > [\mathbf{C}]_{k,k}, \quad (25)$$

then the  $t$ -th distilled model strictly outperforms the  $(t-1)$ -th distilled model in the sense that the  $t$ -th model achieves 100% population accuracy but not the  $(t-1)$ -th model.

*Proof.* This theorem can be proved by analyzing (21) for correctly (clean) vs. incorrectly (noisy)-labeled samples.

**Clean sample:** For the clean sample having  $\hat{y}_i = y_i$ , the prediction of the  $t$ -th distilled model is given by

$$[\mathbf{y}_i^{(t)}]_k = \begin{cases} p^t + (q^t - p^t)[\mathbf{C}]_{y_i, y_i} + (1 - q^t)/K, & k = y_i; \\ (q^t - p^t)[\mathbf{C}]_{y_i, k} + (1 - q^t)/K, & o.w. \end{cases} \quad (26)$$

from (21). Thus, the condition for the student model to correctly classify *all* clean samples, i.e.,  $[\mathbf{y}_i^{(t)}]_{y_i} > [\mathbf{y}_i^{(t)}]_k$  for all  $k \neq y_i$  and all  $y_i \in [K]$ , is given by

$$[\mathbf{C}]_{k,k} > [\mathbf{C}]_{k,k'} - \frac{1}{(q/p)^t - 1}, \quad \forall k, k' (\neq k) \in [K]. \quad (27)$$

**Noisy sample:** For the noisy sample having  $\hat{y}_i \neq y_i$ , the prediction of the  $t$ -th distilled model is given by

$$[\mathbf{y}_i^{(t)}]_k = \begin{cases} (q^t - p^t)[\mathbf{C}]_{y_i, y_i} + (1 - q^t)/K, & k = y_i; \\ p^t + (q^t - p^t)[\mathbf{C}]_{y_i, \hat{y}_i} + (1 - q^t)/K, & k = \hat{y}_i; \\ (q^t - p^t)[\mathbf{C}]_{y_i, k} + (1 - q^t)/K, & o.w. \end{cases} \quad (28)$$

Thus, the condition for a student model to correctly classify all the noisy samples is given by

$$[\mathbf{C}]_{k,k} > [\mathbf{C}]_{k,k'} + \frac{1}{(q/p)^t - 1}, \quad \forall k, k' (\neq k) \in [K]. \quad (29)$$

Note that (29) is a stronger condition than (27). Thus, under (29) the  $t$ -th distilled model achieves 100% accuracy.  $\square$

**Remark 2** (Label noise rate and accuracy of student model). The analysis of the  $t$ -th distilled model reveals the relation between the label noise rate and the accuracy of the student model. Let us assume that the label noise rate is  $c\%$  in the training dataset, and for each class  $k \in [K]$  the portion of samples with the correct label  $k$  is larger than those of any other  $k' \neq k$ , i.e.,  $[\mathbf{C}]_{k,k} > [\mathbf{C}]_{k,k'}$  for any  $k' \neq k$ . Under this condition, (27) is satisfied so that the student model correctly classifies all the clean samples. However, if  $[\mathbf{C}]_{k,k} < [\mathbf{C}]_{k,k'} + \frac{1}{(q/p)^t - 1}$  for some  $k, k' (\neq k)$ , the noisy samples having label  $\hat{y}_i = k'$  are classified to  $k'$  even when the true class is  $y_i = k$ . Thus, the population error rate of the student model is equal to  $100 \times$

$$\sum_{k, k' \in [K], k \neq k'} \frac{[\mathbf{C}]_{k,k'}}{K} \mathbb{1} \left( [\mathbf{C}]_{k,k} < [\mathbf{C}]_{k,k'} + \frac{1}{(q/p)^t - 1} \right) \% \quad (30)$$

If  $[\mathbf{C}]_{k,k} < [\mathbf{C}]_{k,k'} + \frac{1}{(q/p)^t - 1}$  for all  $k, k' (\neq k)$ , then the population error rate of  $l$ -th distilled model for  $l \leq t$  is equal to the label noise rate  $c\%$ .

In Fig. 1b, we compare the classification accuracy of the models as the label corruption rate increases (assuming uniform label corruption across classes) for different number  $t$  of distillation rounds. Note that  $t = 1$  is the accuracy of the teacher model. The solid lines are the results obtained by numerically solving (10) without applying Assm.2 (linearization of softmax function), while the dotted lines are the results from Thm. 1. We can observe that as the distillation round  $t$  increases, the range of label corruption where the student model can achieve 100% accuracy increases, as it gets easier to satisfy the condition (24). Moreover, the dotted lines are aligned well with solid lines, validating our approximation for softmax functions. In Fig. 1c–1d, we also compare how the softmax output  $[\mathbf{y}^{(t)}]_k$  changes for clean/noisy samples as the distillation round  $t$  increases. The dotted lines are from (26) and (28), while solid lines are from numerical calculation without the softmax approximation. For the noisy sample, a few rounds of distillation makes the true label have the highest value in the softmax output, improving the classification performance. As  $t$  increases further, all the outputs converge to a uniform vector.

### 4.3 Comparison between Partial Label Learning and Multi-Round Self-Distillation

We next analyze the condition for the student model with partial label learning to achieve 100% population accuracy and compare this condition with that of the self-distillation.

**Theorem 2.** *Suppose that we have access to the population, i.e.,  $n \rightarrow \infty$ . Under Assumptions 1, 2 and (17), if*

$$[\mathbf{C}]_{k,k} > [\mathbf{C}]_{k,k'}, \quad \forall k, k' (\neq k) \in [K]. \quad (31)$$

*then the student model with partial label learning achieves 100% population accuracy.*

*Proof sketch.* Under the condition (31), the output of the teacher model,  $\mathbf{y}_i^{(1)}$ , has either the highest or the second highest value at the ground-truth label  $y_i$ , as can be shown by (26) and (28). More specifically, the input to the student model from PLL is given by  $\tilde{\mathbf{y}}_i = \frac{1}{2}\mathbf{e}(y_i) + \frac{1}{2}\mathbf{e}(\tilde{y}_i)$  for a clean sample where  $\tilde{y}_i := \arg \max_{k \neq y_i} [\mathbf{C}]_{y_i,k}$ , and  $\tilde{\mathbf{y}}_i = \frac{1}{2}\mathbf{e}(y_i) + \frac{1}{2}\mathbf{e}(\tilde{y}_i)$  for a noisy sample. With these  $\{\tilde{\mathbf{y}}_i\}$ , we can prove that the student model achieves 100% accuracy by analyzing (22). Full proof can be found in Appx. F.2.  $\square$

**Remark 3** (PLL vs. Self-Distillation). The condition (24) for achieving 100% accuracy by the  $t$ -th self-distilled model is strictly stronger than that for PLL (31). Thus, PLL achieves strictly better performance than the self-distilled model (even after multiple rounds) in the high-noise ratio regime where (31) is satisfied but with a small margin so that (24) cannot be satisfied. This can be shown in Fig. 1b.

## 5 Experiment

In this section, we validate our theoretical findings through experimental results on both synthetic and real datasets. We use a two-layer neural network, composed of a linear layer followed by a softmax layer, on the top of a given feature extractor (varying depending on datasets). We conduct experiments for two different label corruption scenarios: symmetric label corruption and asymmetric label corruption. For symmetric label corruption, for a given corruption rate  $\eta \in [0, 1]$ , the label corruption matrix  $\mathbf{C}$  in (23) is defined as  $[\mathbf{C}]_{k,k'} = 1 - \eta$  for  $k' = k$  and  $\frac{\eta}{K-1}$  otherwise. This means that for each label, the probability of no corruption is  $1 - \eta$  and if corruption occurs, the given label is uniformly distributed among the other  $(K - 1)$  labels. For asymmetric label corruption, on the other hand, the label corruption matrix  $\mathbf{C}$  is defined as  $[\mathbf{C}]_{k,k'} = 1 - \eta$  for  $k' = k$ ,  $\frac{2\eta}{K}$  for  $k' = \tilde{k}(k)$  and  $\frac{\eta}{K}$  for  $k' \neq k, \tilde{k}(k)$ . For each label  $k$ , there exists a unique most confusing label  $\tilde{k}(k)$  that occurs with twice larger probability than the other incorrect labels.

### 5.1 Synthetic Dataset Experiment

Following the ResNet architecture He et al. (2016), we generate  $d = 512$  dimensional feature vectors. We select a dataset size of  $Kn = 50,000$  with  $K = 10$  classes. The feature  $\phi(\mathbf{x}_i)$  for sample  $i$  is generated by

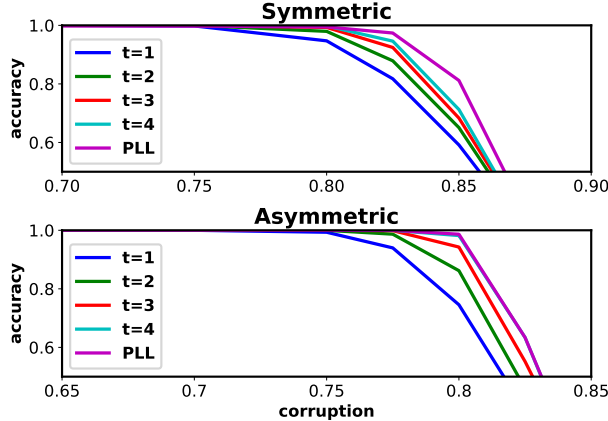


Figure 2: Synthetic experiments on symmetric and asymmetric noise scenarios, with  $\lambda = 2 \times 10^{-6}$ ,  $c = 0.03$ , and  $d = 100$ ; ResNet34 training with CIFAR-100 datasets, where weight decay value is  $\lambda = 2 \times 10^{-7}$ .

	Symmetric				Asymmetric			
	0.7	0.75	0.8	0.85	0.7	0.75	0.8	0.85
$t = 1$	51.17±0.63%	47.65±0.17%	42.74±0.78%	35.31±0.39%	50.80±0.45%	47.73±0.29%	42.67±0.31%	34.89±0.54%
$t = 2$	<b>52.88±0.33%</b>	49.96±0.24%	44.76±0.72%	38.32±0.30%	52.60±0.12%	49.86±0.39%	44.98±0.19%	37.69±0.77%
$t = 3$	52.67±0.39%	49.87±0.24%	44.88±0.51%	38.20±0.35%	52.70±0.22%	49.91±0.11%	45.02±0.45%	38.49±0.86%
$t = 4$	52.71±0.64%	50.34±0.25%	45.25±0.39%	38.42±0.16%	<b>52.79±0.22%</b>	50.02±0.37%	45.43±0.43%	38.35±0.81%
PLL	52.03±0.24%	<b>50.38±0.23%</b>	<b>47.46±0.44%</b>	<b>42.20±0.30%</b>	51.75±0.11%	<b>50.42±0.40%</b>	<b>47.01±0.28%</b>	<b>42.52±0.73%</b>

concatenating the signal part  $\mathbf{v}_{y_i}$  and the noise part  $N(0, \gamma^2 \mathbf{I}_{d-K})$  as follows:

$$\tilde{\phi}(\mathbf{x}_i) = \mathbf{v}_{y_i} \oplus N(0, \gamma^2 \mathbf{I}_{d-K}), \quad \phi(\mathbf{x}_i) = \tilde{\phi}(\mathbf{x}_i) / \|\tilde{\phi}(\mathbf{x}_i)\|$$

Here,  $\mathbf{v}_{y_i}$  represents the feature mean distributed in  $K$ -dimension, while additive Gaussian noise is randomly generated in the  $(d-K)$  dimensions orthogonal to the feature mean space. This approach to feature generation allows us to explore various scenarios of feature correlation by adjusting the mean features  $\{\mathbf{v}_k\}_{k=1}^K$  and the variance  $\gamma^2$ . The mean feature correlation satisfies (17). Further details on the experimental setup are provided in Appendix § B.

Fig. 2 illustrates how the population accuracy of the  $t$ -th distilled model and PLL model change as the label corruption rate increases both for symmetric and asymmetric label noise. We observe that the range of label corruption maintaining 100% accuracy increases as the distillation round increases. Also, our proposed PLL student model outperforms the multi-round distilled models in high noise rates.

## 5.2 Real Dataset Experiments

We conduct experiments with the image classification benchmarks, CIFAR-10/100 Krizhevsky et al. (2009), utilizing PyTorch torchvision library. We use pre-trained ResNet18 and ResNet34 networks He et al. (2016) as feature extractors for CIFAR-10 and CIFAR-100, respectively. We perform linear probing on the pretrained ResNet networks. Table 1 shows the accuracy of student models after  $t$  rounds of self-distillation and that using PLL in the high noise rate ( $\eta \geq 0.7$ ) regime for CIFAR-100. The result for CIFAR-10 is also available in Table 2. We observe an increase in test accuracy as the distillation round increases. Furthermore, we see that PLL student model outperforms other multi-round distillation models in the higher corruption regime. This results validates our theoretical finding in Sec. 4, where we show that self-distillation play a role as label averaging, facilitating the correction of label noise.

## 6 Conclusion

We investigated SD for multi-class classification with CE loss. Through theoretical analysis, we demonstrated that multi-round SD serves as a form of label averaging, enabling the correction of label noises. We also introduced the PLL student model as an effective approach for label refinement. We experimentally validated our claims on both synthetic and real datasets. Our work reveals a novel insight on the effect of SD and also provides a new way of distilling the “dark knowledge” of the teacher, as a candidate set of labels.

## Broader Impact

Our paper theoretically analyzes self-distillation, particularly highlighting its advantages in multi-class classification problems with label noise. Furthermore, we explore the integration of self-distillation with partial label learning, demonstrating its superior performance gains over traditional multi-round self-distillation, especially in high noise rate regimes. This research directly addresses the prevalent challenges in handling real-world data, where acquiring clean and accurately labeled datasets is often difficult and costly. By enhancing our understanding of knowledge distillation and self distillation, we also provide the way for the development of more efficient models, capable of matching the performance of their larger and more complex counterparts, which is especially beneficial in scenarios with limited resources.

## References

- Allen-Zhu, Z. and Li, Y. Towards understanding ensemble, knowledge distillation and self-distillation in deep learning. In *The Eleventh International Conference on Learning Representations*, 2022.
- Asif, U., Tang, J., and Harrer, S. Ensemble knowledge distillation for learning improved and efficient networks. *arXiv preprint arXiv:1909.08097*, 2019.
- Chebatar, Y. and Waters, A. Distilling knowledge from ensembles of neural networks for speech recognition. In *Interspeech*, pp. 3439–3443, 2016.
- Chen, P., Liu, S., Zhao, H., and Jia, J. Distilling knowledge via knowledge review. In *Proceedings of the IEEE/CVF Conference on Computer Vision and Pattern Recognition*, pp. 5008–5017, 2021.
- Cour, T., Sapp, B., and Taskar, B. Learning from partial labels. *The Journal of Machine Learning Research*, 12:1501–1536, 2011.
- Cui, J., Kingsbury, B., Ramabhadran, B., Saon, G., Sercu, T., Audhkhasi, K., Sethy, A., Nussbaum-Thom, M., and Rosenberg, A. Knowledge distillation across ensembles of multilingual models for low-resource languages. In *2017 IEEE International Conference on Acoustics, Speech and Signal Processing (ICASSP)*, pp. 4825–4829. IEEE, 2017.
- Das, R. and Sanghavi, S. Understanding self-distillation in the presence of label noise. In *Proceedings of the 40th International Conference on Machine Learning*, 2023.
- Dong, B., Hou, J., Lu, Y., and Zhang, Z. Distillation  $\approx$  early stopping? harvesting dark knowledge utilizing anisotropic information retrieval for overparameterized neural network. *arXiv preprint arXiv:1910.01255*, 2019.
- Furlanello, T., Lipton, Z., Tschannen, M., Itti, L., and Anandkumar, A. Born again neural networks. In *International Conference on Machine Learning*, pp. 1607–1616. PMLR, 2018.
- He, K., Zhang, X., Ren, S., and Sun, J. Deep residual learning for image recognition. In *Proceedings of the IEEE conference on computer vision and pattern recognition*, pp. 770–778, 2016.

- Hinton, G., Vinyals, O., and Dean, J. Distilling the knowledge in a neural network. *arXiv preprint arXiv:1503.02531*, 2015.
- Ji, G. and Zhu, Z. Knowledge distillation in wide neural networks: Risk bound, data efficiency and imperfect teacher. *Advances in Neural Information Processing Systems*, 33:20823–20833, 2020.
- Krizhevsky, A., Hinton, G., et al. Learning multiple layers of features from tiny images. 2009.
- Lian, Z., Xu, M., Chen, L., Sun, L., Liu, B., and Tao, J. Arnet: Automatic refinement network for noisy partial label learning. *arXiv preprint arXiv:2211.04774*, 2022.
- Liu, X., He, P., Chen, W., and Gao, J. Improving multi-task deep neural networks via knowledge distillation for natural language understanding. *arXiv preprint arXiv:1904.09482*, 2019.
- Lopez-Paz, D., Bottou, L., Schölkopf, B., and Vapnik, V. Unifying distillation and privileged information. *arXiv preprint arXiv:1511.03643*, 2015.
- Lv, J., Xu, M., Feng, L., Niu, G., Geng, X., and Sugiyama, M. Progressive identification of true labels for partial-label learning. In *international conference on machine learning*, pp. 6500–6510. PMLR, 2020.
- Lyu, G., Feng, S., Wang, T., Lang, C., and Li, Y. Gm-pll: Graph matching based partial label learning. *IEEE Transactions on Knowledge and Data Engineering*, 33(2):521–535, 2019.
- Miles, R., Rodriguez, A. L., and Mikolajczyk, K. Information theoretic representation distillation. *arXiv preprint arXiv:2112.00459*, 2021.
- Mobahi, H., Farajtabar, M., and Bartlett, P. Self-distillation amplifies regularization in hilbert space. *Advances in Neural Information Processing Systems*, 33:3351–3361, 2020.
- Phuong, M. and Lampert, C. Towards understanding knowledge distillation. In *International conference on machine learning*, pp. 5142–5151. PMLR, 2019.
- Romero, A., Ballas, N., Kahou, S. E., Chassang, A., Gatta, C., and Bengio, Y. Fitnets: Hints for thin deep nets. *arXiv preprint arXiv:1412.6550*, 2014.
- Tian, Y., Krishnan, D., and Isola, P. Contrastive representation distillation. In *International Conference on Learning Representations*, 2019.
- Wang, D.-B., Li, L., and Zhang, M.-L. Adaptive graph guided disambiguation for partial label learning. In *Proceedings of the 25th ACM SIGKDD International Conference on Knowledge Discovery & Data Mining*, pp. 83–91, 2019.
- Wang, H., Xiao, R., Li, Y., Feng, L., Niu, G., Chen, G., and Zhao, J. Pico: Contrastive label disambiguation for partial label learning. In *International Conference on Learning Representations*, 2021.
- Wang, H., Xiao, R., Li, Y., Feng, L., Niu, G., Chen, G., and Zhao, J. Pico+: Contrastive label disambiguation for robust partial label learning. *IEEE Transactions on Pattern Analysis and Machine Intelligence*, 2023a.
- Wang, Y., Cheng, L., Duan, M., Wang, Y., Feng, Z., and Kong, S. Improving knowledge distillation via regularizing feature norm and direction. *arXiv preprint arXiv:2305.17007*, 2023b.
- Xu, M., Lian, Z., Feng, L., Liu, B., and Tao, J. Dali: Dynamically adjusted label importance for noisy partial label learning. *arXiv preprint arXiv:2301.12077*, 2023.
- Xu, N., Lv, J., and Geng, X. Partial label learning via label enhancement. In *Proceedings of the AAAI Conference on artificial intelligence*, volume 33, pp. 5557–5564, 2019.

Zhang, L., Song, J., Gao, A., Chen, J., Bao, C., and Ma, K. Be your own teacher: Improve the performance of convolutional neural networks via self distillation. In *Proceedings of the IEEE/CVF international conference on computer vision*, pp. 3713–3722, 2019.

Zhao, B., Cui, Q., Song, R., Qiu, Y., and Liang, J. Decoupled knowledge distillation. In *Proceedings of the IEEE/CVF Conference on computer vision and pattern recognition*, pp. 11953–11962, 2022.

## A Justification of Assumptions

In this section, we provide empirical justifications for the assumptions we have imposed in the theoretical analysis.

### A.1 Justification of Feature Correlation Assumption (Assumption 1)

In Assumption 1, we argue that the similarity between two features is determined by the corresponding true label pairs, i.e.,

$$\langle \phi(\mathbf{x}_i), \phi(\mathbf{x}_j) \rangle = \omega(y_i, y_j) \text{ for } i \neq j. \quad (32)$$

We empirically demonstrate the validity of this assumption on a real dataset, CIFAR-100. In our real-world dataset experiments in Sec. 5.2, we utilized the pre-trained ResNet-34 for the CIFAR-100 dataset to extract the features. The corresponding feature correlation map is described in Fig. 3a. We observe that the diagonal elements of the feature correlation matrix are higher than the off-diagonal elements. The diagonal entries have mean 0.54 and standard deviation 0.12, while the off-diagonal entries have mean 0.45 and standard deviation 0.11. This observation supports the validity of our Assumption 1 that the feature correlation between two samples is governed by the corresponding true label pairs, and also further assumption in (17) that any two instances of the same ground-truth class has a higher feature correlation than those between instances from different classes.

### A.2 Justification of Softmax Approximation Assumption (Assumption 2)

In Assumption 2, we approximate the softmax function  $\sigma(\mathbf{v})$  to the linear function  $1/K + \mathbf{v}/K$ , assuming a small enough magnitude of  $\mathbf{v}$ . To justify our approximation, let us recall the equation for  $\boldsymbol{\alpha}_i$ :

$$Kn\lambda\boldsymbol{\alpha}_i = \mathbf{e}(\hat{y}_i) - \sigma((1 - \omega(y_i, y_i))\boldsymbol{\alpha}_i + \mathbf{s}_\alpha(y_i)), \quad (33)$$

where  $\mathbf{s}_\alpha(y_i) = \sum_{j=1}^{Kn} \omega(y_i, y_j)\boldsymbol{\alpha}_j$ .

We numerically validate Assumption 2, by analyzing the softmax approximation error. The softmax approximation error is defined as the maximum difference ( $\ell_\infty$ -norm) between the softmax outputs derived in Lemma 1, based on the linear approximation of the softmax, and the outputs obtained by numerically solving (33) for  $\{\boldsymbol{\alpha}_i\}$  where  $\mathbf{y}_i^{(T)} = \sigma((1 - \omega(y_i, y_i))\boldsymbol{\alpha}_i + \mathbf{s}_\alpha(y_i))$ . We assume the feature correlation  $\omega(y_i, y_i)$  is given by (17) and the dataset has symmetric label corruption with rate  $\eta = 0.5$ . We set  $K = 10$ ,  $\lambda = 10^{-4}$ ,  $c = 0.03$ ,  $d = 0.01$ . We analyze the softmax error as the number of samples increases. As shown in Fig. 3b, the softmax error becomes negligible, especially as the number of samples exceeds  $10^4$ .

## B Experimental Details

In this section, we provide the details of the experiments presented in Sec. 5.

### B.1 Generation of Synthetic Dataset

In the synthetic experiment, our feature vector  $\phi(\mathbf{x}_i)$  is defined as follows:

$$\tilde{\phi}(\mathbf{x}_i) = \mathbf{v}_{y_i} \oplus N(0, \gamma^2 \mathbf{I}_{d-K}), \quad \phi(\mathbf{x}_i) = \frac{\tilde{\phi}(\mathbf{x}_i)}{\|\tilde{\phi}(\mathbf{x}_i)\|} \quad (34)$$

Hence, the feature correlation between two feature  $\langle \phi(\mathbf{x}_i), \phi(\mathbf{x}_j) \rangle$  can be written as follows:

$$\langle \phi(\mathbf{x}_i), \phi(\mathbf{x}_j) \rangle = \frac{\langle \mathbf{v}_{y_i}, \mathbf{v}_{y_j} \rangle + \langle N(0, \gamma^2 \mathbf{I}_{d-K}), N(0, \gamma^2 \mathbf{I}_{d-K}) \rangle}{\sqrt{\|\mathbf{v}_{y_i}\|^2 + (d-K)\gamma^2} \sqrt{\|\mathbf{v}_{y_j}\|^2 + (d-K)\gamma^2}} \quad (35)$$

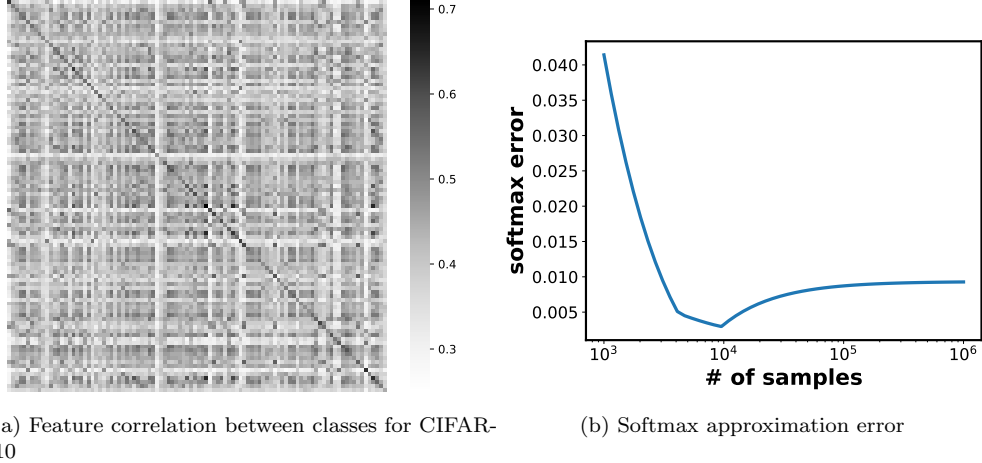


Figure 3: (a) Feature correlation map between classes for CIFAR-100 dataset, where the features are extracted from the pre-trained ResNet34. The diagonal entries (sample-class instances) have mean 0.54 and standard deviation 0.12, while the off-diagonal entries (different-class instances) have mean 0.45 and standard deviation 0.11. (b) We plot the softmax approximation error as the number of samples increases. We use  $K = 10$ ,  $\lambda = 10^{-4}$ ,  $c = 0.03$ ,  $d = 0.01$ , and impose the symmetric noise with  $\eta = 0.5$ .

After fixing  $\|\mathbf{v}_k\| = 1$  for all  $k$ , we have

$$\begin{aligned}\mathbb{E}[\langle \phi(\mathbf{x}_i), \phi(\mathbf{x}_j) \rangle] &= \frac{\langle \mathbf{v}_{y_i}, \mathbf{v}_{y_j} \rangle}{1 + (d - K)\gamma^2}, \\ \text{Var}(\langle \phi(\mathbf{x}_i), \phi(\mathbf{x}_j) \rangle) &= \frac{(d - K)\gamma^4}{1 + (d - K)\gamma^2}.\end{aligned}\tag{36}$$

Hence, by adjusting the feature mean  $\mathbf{v}$  and the parameter  $\gamma$  appropriately, we can obtain the desired feature correlation map. Furthermore, in making  $\mathbb{E}[\langle \phi(\mathbf{x}_i), \phi(\mathbf{x}_j) \rangle] = c$  for some  $c > 0$ , increasing the feature dimension  $d$  leads to a decrease of  $\gamma$ , resulting in a decrease of  $\text{Var}(\langle \phi(\mathbf{x}_i), \phi(\mathbf{x}_j) \rangle)$ . Therefore, with a sufficiently large feature dimension  $d$ , we can generate a feature dataset that satisfies our Assumption 1. The following shows the method for selecting  $\mathbf{v}_{y_i}$  in different feature correlation scenarios.

**CASE I** (Instances of different labels are uncorrelated): For each class, we randomly select an axis and define the feature mean  $\mathbf{v}_k$  as the unit vector in that direction. Then, the feature correlation  $\omega(y_i, y_j)$  can be expressed as

$$\omega(y_i, y_j) \approx \mathbb{E}[\langle \phi(\mathbf{x}_i), \phi(\mathbf{x}_j) \rangle] = \begin{cases} \frac{1}{1 + (d - K)\gamma^2}, & y_i = y_j \\ 0, & y_i \neq y_j \end{cases}\tag{37}$$

**CASE II** (Instances of different labels are correlated): We choose one axis and denote its unit vector as  $\mathbf{w}$ . Subsequently, we randomly select a unit vector  $\mathbf{u}_{y_i}$  for each class  $y_i$ . Here,  $\mathbf{v}_{y_i}$  is the linear combination of  $\mathbf{w}$  and  $\mathbf{u}_{y_i}$ , given as

$$\mathbf{v}_{y_i} = \xi \mathbf{w} + \sqrt{1 - \xi^2} \mathbf{u}_{y_i}, \quad \xi \in (0, 1)\tag{38}$$

Then, the feature correlation  $\omega(y_i, y_j)$  can be expressed as

$$\omega(y_i, y_j) \approx \mathbb{E}[\langle \phi(\mathbf{x}_i), \phi(\mathbf{x}_j) \rangle] = \begin{cases} \frac{1}{1 + (d - K)\gamma^2}, & y_i = y_j \\ \frac{\xi^2}{1 + (d - K)\gamma^2}, & y_i \neq y_j \end{cases}\tag{39}$$



## B.2 Training

We train a two-layer network consisting of a linear layer and a softmax layer. Our loss function is defined as the cross-entropy between the softmax output of the teacher model and the softmax output of the student model. To mitigate uncertainty, we conduct three repeated runs for all experiments. We perform a grid search over learning rates, in the set  $\{0.1, 0.05, 0.01\}$ . Each model is trained for 200 epochs, employing the SGD optimizer with a momentum value of 0.9. Our neural networks are trained using NVIDIA-GeForce 3090 GPUs.

## B.3 Choosing appropriate $\lambda$

In real experiments, we extract features from the CIFAR-10 and CIFAR-100 datasets using pretrained ResNet18 and ResNet34 models, respectively. In this process, the average feature correlation within the same class is about 0.54, while the average feature correlation between different classes is about 0.4. Recall the definition of  $p$  and  $q$  from (19):

$$p := 1 - \frac{K^2 n \lambda}{K^2 n \lambda + 1 - c}, \tag{40}$$

$$q := 1 - \frac{K^2 n \lambda}{K^2 n \lambda + 1 - c + n(c - d)} \tag{41}$$

In this setting, we visualize the variation of the  $q/p$  ratio as  $\lambda$  changes, to find an appropriate  $\lambda$ . When the  $q/p$  ratio is too small or too large, it becomes hard to demonstrate the effect of distillation from Thm. 1. Through Fig. 4, we observe that to obtain a  $q/p$  ratio near 2,  $\lambda$  should be selected near  $10^{-6}$  for CIFAR-10 and near  $10^{-7}$  for CIFAR-100. Hence, in the main text, we set the  $\lambda$  to  $2 \times 10^{-6}$  for CIFAR-10 and  $2 \times 10^{-7}$  for CIFAR-100 to demonstrate the effect of distillation. We present additional results for various values of  $\lambda$  in the Appendix §G.

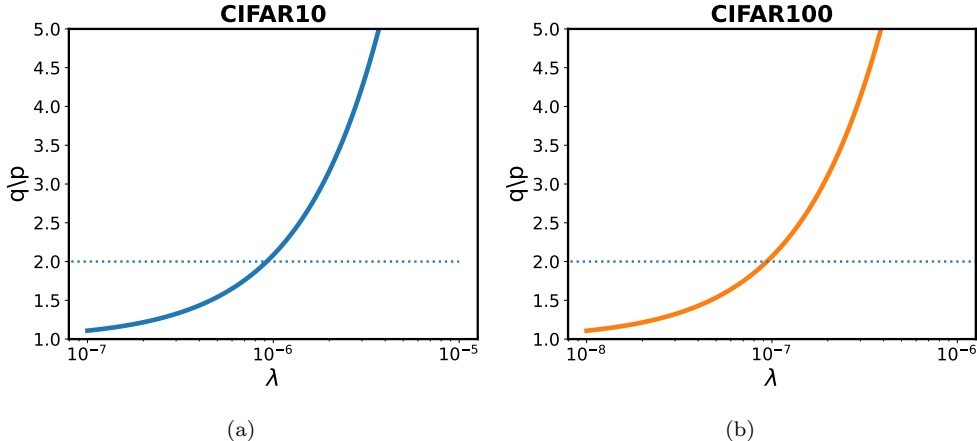


Figure 4: Variation of  $q/p$  with changing weight decay  $\lambda$ .

## C Experimental Results on CIFAR-10

We conduct experiments with the image classification benchmarks, CIFAR-10/100 Krizhevsky et al. (2009), utilizing PyTorch torchvision library. We use pre-trained ResNet18 and ResNet34 networks He et al. (2016) as feature extractors for CIFAR-10 and CIFAR-100, respectively. We perform linear probing on the pretrained

ResNet networks. Table 2 shows the accuracy of student model with  $t$  round self-distillation and that using PLL in the high label corruption ( $\eta$ ) regime for CIFAR-10. The result for CIFAR-100 is available in Table 1. We see that PLL student model outperforms other multi-round distillation models in the higher corruption regime.

Table 2: ResNet18 training with CIFAR-10 datasets, where weight decay value is  $\lambda = 2 \times 10^{-6}$ .

Model	Symmetric				Asymmetric			
	0.7	0.75	0.8	0.85	0.7	0.75	0.8	0.85
$t = 1$	68.06±0.64%	60.82±0.13%	49.72±2.03%	30.65±1.43%	64.97±0.27%	56.60±0.54%	42.87±2.13%	24.43±0.56%
$t = 2$	<b>70.75±1.31%</b>	63.70±0.52%	52.54±2.41%	32.14±1.89%	67.70±0.62%	<b>58.33±0.97%</b>	41.91±1.87%	21.99±1.46%
$t = 3$	70.71±1.20%	64.08±0.77%	52.45±2.01%	32.23±1.70%	<b>68.02±0.95%</b>	58.19±1.14%	41.95±1.92%	21.88±1.25%
$t = 4$	70.70±1.46%	63.90±0.44%	52.55±1.84%	32.28±1.85%	67.85±0.86%	58.25±1.20%	42.16±1.51%	21.86±1.49%
PLL	69.57±0.81%	<b>65.27±1.17%</b>	<b>57.84±2.35%</b>	<b>38.04±2.67%</b>	62.72±0.90%	56.86±0.31%	<b>44.98±0.46%</b>	<b>24.86±1.23%</b>

## D Proof

### D.1 Effect of Temperature Scaling

Let  $\mathbf{y}_i^{(t)}$  represent the output of the  $t$ -th distilled model for the  $i$ -th sample. The objective function for the  $t$ -th distilled model  $f^{(t)}(\boldsymbol{\theta})$ , scaled by temperature  $\tau$  is given by

$$f^{(t)}(\boldsymbol{\theta}) = \frac{\tau^2}{Kn} \sum_{i=1}^{Kn} \text{CE}(\mathbf{y}_i^{(t-1)}, \sigma^\tau(\boldsymbol{\theta}^\top \phi(\mathbf{x}_i))) + \frac{\lambda \|\boldsymbol{\theta}\|_F^2}{2}, \quad (42)$$

for  $t \in \mathbb{N}$ . Then, the optimal  $\boldsymbol{\theta}$ , denoted as  $\boldsymbol{\theta}^*$  satisfies

$$\boldsymbol{\theta}^{*\top} = \tau \sum_{i=1}^{Kn} \underbrace{\frac{1}{Kn\lambda} (\mathbf{y}_i^{(t-1)} - \mathbf{y}_i^{(t)})}_{:=\boldsymbol{\alpha}_i^{(t)}} \phi(\mathbf{x}_i)^\top = \tau \sum_{i=1}^{Kn} \boldsymbol{\alpha}_i^{(t)} \phi(\mathbf{x}_i)^\top. \quad (43)$$

Substitute the optimal  $\boldsymbol{\theta}$  yields

$$\begin{aligned} Kn\lambda \boldsymbol{\alpha}_i^{(t)} &= \mathbf{y}_i^{(t-1)} - \mathbf{y}_i^{(t)} \\ &= \mathbf{y}_i^{(t-1)} - \sigma^\tau \left( \tau \sum_{j=1}^{Kn} \boldsymbol{\alpha}_j^{(t)} \phi(\mathbf{x}_j)^\top \phi(\mathbf{x}_i) \right) \\ &= \mathbf{y}_i^{(t-1)} - \sigma^1 \left( (1 - \omega(y_i, y_i)) \boldsymbol{\alpha}_i^{(t)} + \sum_{i=1}^{Kn} \omega(y_i, y_j) \boldsymbol{\alpha}_j^{(t)} \right). \end{aligned}$$

Here, one can see that applying temperature scaling does not affect the prediction  $\mathbf{y}_i^{(t)}$ .

### D.2 Proof of Lemma 1

Recall (10):

$$(K^2 n \lambda + 1 - \omega(y_i, y_i)) \boldsymbol{\alpha}^{(t)} = \mathbf{y}_i^{(t-1)} - \sigma \left( (1 - \omega(y_i, y_i)) \boldsymbol{\alpha}_i^{(t)} + \mathbf{s}_\alpha(y_i) \right). \quad (44)$$

By applying the softmax approximation (Assumption 2), we have

$$(K^2 n \lambda + 1 - \omega(y_i, y_i)) \boldsymbol{\alpha}_i^{(t)} = K \mathbf{y}_i^{(t-1)} - \mathbf{s}_\alpha^{(t)}(y_i) - \mathbf{1}_K. \quad (45)$$

For the simplicity, let us define two matrices  $\mathbf{Y}^{(t)} \in \mathbb{R}^{K \times Kn}$  and  $\mathbf{P} \in \mathbb{R}^{K \times Kn}$ :

$$\mathbf{Y}^{(t)} := [\mathbf{y}_1^{(t)}, \dots, \mathbf{y}_{Kn}^{(t)}], \quad (46)$$

and

$$\mathbf{P} := [\mathbf{e}(y_1), \dots, \mathbf{e}(y_{Kn})]. \quad (47)$$

Note that  $\mathbf{Y}^{(0)} = [\mathbf{e}(\hat{y}_1), \dots, \mathbf{e}(\hat{y}_{Kn})]$ . Then, we have

$$\mathbf{Y}^{(t)} \mathbf{P}^\top = \left[ \sum_{\{j: y_j=1\}} \mathbf{y}_j^{(t)}, \dots, \sum_{\{j: y_j=K\}} \mathbf{y}_j^{(t)} \right] \in \mathbb{R}^{K \times K}. \quad (48)$$

Also, because of the balanced true-labels of the dataset, we have

$$\mathbf{P} \mathbf{P}^\top = \mathbf{D}(|\{j : y_j = 1\}|, \dots, |\{j : y_j = K\}|) = n \mathbf{I}_{K \times K} \in \mathbb{R}^{K \times K}, \quad (49)$$

where  $\mathbf{D}(\mathbf{v})$  is the diagonal matrix with elements composed of vector  $\mathbf{v}$ .

**Lemma 3.** Consider three  $K \times K$  matrices  $\mathbf{A}$ ,  $\mathbf{B}$ , and  $\mathbf{C}$  satisfying the equation

$$\mathbf{A}[:, j] = \sum_{k=1}^K \mathbf{B}[j, k] \mathbf{C}[:, k].$$

Then,

$$\mathbf{A} = \mathbf{C} \mathbf{B}^\top. \quad (50)$$

*Proof.*

$$\mathbf{A}[i, j] = \sum_{k=1}^K \mathbf{B}[j, k] \mathbf{C}[i, k] = \sum_{k=1}^K \mathbf{C}[i, k] \mathbf{B}^\top[k, j]$$

Thus,  $\mathbf{A} = \mathbf{C} \mathbf{B}^\top$ . □

Define a matrix  $\mathbf{W} \in \mathbb{R}^{K \times K}$  as

$$\mathbf{W}[x, y] = \frac{\omega(x, y)}{K^2 n \lambda + 1 - \omega(x, x)}, \quad (51)$$

Then,  $\mathbf{s}_\alpha^{(t)}(y_i)$  can be formulated as

$$\begin{aligned} \mathbf{s}_\alpha^{(t)}(y_i) &= \sum_{j=1}^{Kn} \frac{\omega(y_i, y_j)}{K^2 n \lambda + 1 - \omega(y_i, y_i)} \left( K \mathbf{y}_j^{(t-1)} - \mathbf{s}_\alpha^{(t)}(y_j) - \mathbf{1}_K \right) \\ &= \sum_{j=1}^{Kn} \mathbf{W}[y_i, y_j] \left( K \mathbf{y}_j^{(t-1)} - \mathbf{s}_\alpha^{(t)}(y_j) - \mathbf{1}_K \right) \\ &= \sum_{j=1}^{Kn} K \mathbf{W}[y_i, y_j] \mathbf{y}_j^{(t-1)} - \sum_{j=1}^{Kn} \mathbf{W}[y_i, y_j] \left( \mathbf{s}_\alpha^{(t)}(y_j) + \mathbf{1}_K \right) \end{aligned}$$

We can use Lemma 3 to simplify the first sum as follows:

$$\begin{aligned} \sum_{j=1}^{Kn} K \mathbf{W}[y_i, y_j] \mathbf{y}_j^{(t-1)} &= \sum_{y_j=1}^K K \mathbf{W}[y_i, y_j] \sum_{\{k: y_k=y_j\}} \mathbf{y}_k^{(t-1)} \\ &= \sum_{y_j=1}^K K \mathbf{W}[y_i, y_j] (\mathbf{Y}^{(t-1)} \mathbf{P}^\top)[:, y_j] \\ &= K \mathbf{Y}^{(t-1)} \mathbf{P}^\top \mathbf{W}^\top[:, y_i] \end{aligned}$$

Additionally, let us define  $\mathbf{S}_\alpha^{(t)} \in \mathbb{R}^{K \times K}$  as

$$\mathbf{S}_\alpha^{(t)} = [\mathbf{s}_\alpha^{(t)}(1), \dots, \mathbf{s}_\alpha^{(t)}(K)]. \quad (52)$$

Then, the second sum can be simplified as

$$\begin{aligned} \sum_{j=1}^{Kn} \mathbf{W}[y_i, y_j] (\mathbf{s}_\alpha^{(t)}(y_j) + \mathbf{1}_K) &= \sum_{y_j=1}^K \mathbf{W}[y_i, y_j] |\{k : y_k = y_j\}| (\mathbf{s}_\alpha^{(t)}(y_j) + \mathbf{1}_K) \\ &= \sum_{j=1}^K n \mathbf{W}[y_i, y_j] \left( \mathbf{S}_\alpha^{(t)} + \mathbf{1}_{K \times K} \right)[:, y_j] \\ &= n (\mathbf{S}_\alpha^{(t)} + \mathbf{1}_{K \times K}) \mathbf{W}^\top[:, y_i] \end{aligned}$$

Finally, since  $\mathbf{s}_\alpha^{(t)}(y_i) = \mathbf{S}_\alpha^{(t)}[:, y_i]$ , we obtain an equation for  $\mathbf{S}_\alpha^{(t)}$  by combining two sums.

$$\mathbf{S}_\alpha^{(t)} = K \mathbf{Y}^{(t-1)} \mathbf{P}^\top \mathbf{W}^\top - n (\mathbf{S}_\alpha^{(t)} + \mathbf{1}_{K \times K}) \mathbf{W}^\top$$

and

$$\mathbf{S}_\alpha^{(t)} = K \mathbf{Y}^{(t-1)} \mathbf{P}^\top \mathbf{W}^\top (\mathbf{I} + n \mathbf{W}^\top)^{-1} - n \mathbf{1}_{K \times K} \mathbf{W}^\top (\mathbf{I} + n \mathbf{W}^\top)^{-1}. \quad (53)$$

Note that  $\mathbf{W}^\top (\mathbf{I} + n \mathbf{W}^\top)^{-1}$  satisfies

$$\begin{aligned} (\mathbf{I} + n \mathbf{W}^\top) (\mathbf{I} + n \mathbf{W}^\top)^{-1} &= \mathbf{I} \\ n \mathbf{W}^\top (\mathbf{I} + n \mathbf{W}^\top)^{-1} &= \mathbf{I} - (\mathbf{I} + n \mathbf{W}^\top)^{-1} \end{aligned}$$

From here, we can compute  $\mathbf{y}_i^{(t)}$  as

$$\begin{aligned} \mathbf{y}_i^{(t)} &= \mathbf{y}_i^{(t-1)} - Kn\lambda \boldsymbol{\alpha}_i \\ &= \mathbf{y}_i^{(t-1)} - \frac{Kn\lambda}{K^2n\lambda + 1 - \omega(y_i, y_i)} (K \mathbf{y}_i^{(t-1)} - \mathbf{s}_\alpha^{(t)}(y_i) - \mathbf{1}_K) \\ &= (1 - Kc(y_i)) \mathbf{y}_i^{(t-1)} + c(y_i) \mathbf{s}_\alpha^{(t)}(y_i) + c(y_i) \mathbf{1}_K. \end{aligned}$$

where  $c(y_i)$  is defined as follows:

$$c(y_i) := \frac{Kn\lambda}{K^2n\lambda + 1 - \omega(y_i, y_i)} \quad (54)$$

Let us define a vector  $\mathbf{v}$  as

$$\mathbf{v} = [c(1), \dots, c(K)] \in \mathbb{R}^K. \quad (55)$$

Note that  $\mathbf{v}$  is independent of  $t$ . Then,  $\mathbf{Y}^{(t)}$  satisfies the following equation:

$$\mathbf{Y}^{(t)} = \mathbf{Y}^{(t-1)} (\mathbf{I} - K \mathbf{D}(\mathbf{v} \mathbf{P})) + \mathbf{S}_\alpha^{(t)} \mathbf{D}(\mathbf{v}) \mathbf{P} + \mathbf{1}_{K \times K} \mathbf{D}(\mathbf{v}) \mathbf{P}. \quad (56)$$

After substituting  $\mathbf{S}_\alpha^{(t)}$ , we have

$$\begin{aligned} \mathbf{Y}^{(t)} &= \mathbf{Y}^{(t-1)} \{ \mathbf{I} - K \mathbf{D}(\mathbf{v} \mathbf{P}) + K \mathbf{P}^\top \mathbf{W}^\top (\mathbf{I} + n \mathbf{W}^\top)^{-1} \mathbf{D}(\mathbf{v}) \mathbf{P} \\ &\quad - n \mathbf{1}_{K \times K} \mathbf{W}^\top (\mathbf{I} + n \mathbf{W}^\top)^{-1} \mathbf{D}(\mathbf{v}) \mathbf{P} + \mathbf{1}_{K \times K} \mathbf{D}(\mathbf{v}) \mathbf{P} \} \\ &= \mathbf{Y}^{(t-1)} (\mathbf{I} - K \mathbf{B}) + \mathbf{C}, \end{aligned}$$

where  $\mathbf{B}$  and  $\mathbf{C}$  are given in terms of

$$\mathbf{B} = \mathbf{D}(\mathbf{v} \mathbf{P}) - \mathbf{P}^\top \mathbf{W}^\top (\mathbf{I} + n \mathbf{W}^\top)^{-1} \mathbf{D}(\mathbf{v}) \mathbf{P} \quad (57)$$

$$\mathbf{C} = \mathbf{1}_{K \times K} (\mathbf{I} + n \mathbf{W}^\top)^{-1} \mathbf{D}(\mathbf{v}) \mathbf{P} \quad (58)$$

Please note that  $\mathbf{B}$  and  $\mathbf{C}$  are only the function of  $\omega(i, j)$  and  $\lambda$ , which is invariant as  $t$  changes.

**Lemma 4.**

$$\mathbf{C}\mathbf{B}^{-1} = \mathbf{1}_{K \times Kn}. \quad (59)$$

*Proof.* Let us show  $\mathbf{1}_{K \times Kn}\mathbf{B}$ . We use the following facts:

$$\mathbf{1}_{K \times Kn}\mathbf{D}(\mathbf{v}\mathbf{P}) = [c(y_1)\mathbf{1}_K, \dots, c(y_{Kn})\mathbf{1}_K] = \mathbf{1}_{K \times K}\mathbf{D}(\mathbf{v})\mathbf{P},$$

and

$$\mathbf{1}_{K \times Kn}\mathbf{P}^\top = n\mathbf{1}_{K \times K}.$$

Hence, we can compute  $\mathbf{1}_{K \times Kn}\mathbf{B}$  as follows:

$$\begin{aligned} \mathbf{1}_{K \times Kn}\mathbf{B} &= \mathbf{1}_{K \times Kn}\mathbf{D}(\mathbf{v}\mathbf{P}) - \mathbf{1}_{K \times Kn}\mathbf{P}^\top\mathbf{W}^\top(\mathbf{I} + n\mathbf{W}^\top)^{-1}\mathbf{D}(\mathbf{v})\mathbf{P} \\ &= \mathbf{1}_{K \times K}\mathbf{D}(\mathbf{v})\mathbf{P} - n\mathbf{1}_{K \times K}\mathbf{W}^\top(\mathbf{I} + n\mathbf{W}^\top)^{-1}\mathbf{D}(\mathbf{v})\mathbf{P} \\ &= \mathbf{1}_{K \times K}(\mathbf{I} - \mathbf{W}^\top(\mathbf{I} + n\mathbf{W}^\top)^{-1})\mathbf{D}(\mathbf{v})\mathbf{P} \\ &= \mathbf{C} \end{aligned}$$

Thus, we have  $\mathbf{C}\mathbf{B}^{-1} = \mathbf{1}_{K \times Kn}$ . □

Finally, we can derive a closed form for  $\mathbf{Y}^{(t)}$ :

$$\mathbf{Y}^{(t)} = \left( \mathbf{Y}^{(0)} - \frac{1}{K}\mathbf{1}_{K \times Kn} \right) (\mathbf{I} - \mathbf{K}\mathbf{B})^t + \frac{1}{K}\mathbf{1}_{K \times Kn}, \quad (60)$$

where  $\mathbf{B}$  is defined in (57).

Similarly, we can show that

$$\mathbf{Y}^{(P)} = \left( \bar{\mathbf{Y}} - \frac{1}{K}\mathbf{1}_{K \times Kn} \right) (\mathbf{I}_{Kn} - \mathbf{K}\mathbf{B}) + \frac{1}{K}\mathbf{1}_{K \times Kn}, \quad (61)$$

where  $\bar{\mathbf{Y}} = [\bar{y}_1, \dots, \bar{y}_{Kn}]$  for the output  $\mathbf{Y}^{(P)}$  of the student model with PLL using input  $\bar{\mathbf{Y}} = [\bar{y}_1, \dots, \bar{y}_{Kn}]$ .

## E Proof of Lemma 2 and Closed Form Solutions for Other Feature Correlations

Recall (15), the closed-form solution for  $\mathbf{Y}^{(t)}$ :

$$\mathbf{Y}^{(t)} = \left( \mathbf{Y}^{(0)} - \frac{1}{K}\mathbf{1}_{K \times Kn} \right) (\mathbf{I}_{Kn} - \mathbf{K}\mathbf{B})^t + \frac{1}{K}\mathbf{1}_{K \times Kn}, \quad (62)$$

where  $\mathbf{B}$  and  $\mathbf{C}$  are given as

$$\mathbf{B} = \mathbf{D}(\mathbf{v}\mathbf{P}) - \mathbf{P}^\top\mathbf{W}^\top(\mathbf{I} + n\mathbf{W}^\top)^{-1}\mathbf{D}(\mathbf{v})\mathbf{P}, \quad (63)$$

$$\mathbf{C} = \mathbf{1}_{K \times K}(\mathbf{I} + n\mathbf{W}^\top)^{-1}\mathbf{D}(\mathbf{v})\mathbf{P}. \quad (64)$$

In this section, we compute  $\mathbf{B}$  and  $\mathbf{C}$  for the diverse feature correlation scenarios.

### E.1 Most Simple Case: Constant Correlation $c$

At first, we begin with the most fundamental scenario, where  $\omega(y_i, y_j)$  is defined as

$$\omega(y_i, y_j) = \begin{cases} c, & y_i = y_j \\ 0, & y_i \neq y_j. \end{cases} \quad (65)$$

Here,  $\mathbf{B}$  can be computed as

$$\begin{aligned}
\mathbf{B} &= \mathbf{D}(\mathbf{v}\mathbf{P}) - \mathbf{P}^\top \mathbf{W}^\top (\mathbf{I} + n\mathbf{W}^\top)^{-1} \mathbf{D}(\mathbf{v})\mathbf{P} \\
&= \frac{Kn\lambda}{K^2n\lambda + 1 - c} \mathbf{I} - \frac{c}{K^2n\lambda + 1 - c} \frac{1}{1 + \frac{nc}{K^2n\lambda + 1 - c}} \frac{Kn\lambda}{K^2n\lambda + 1 - c} \mathbf{P}^\top \mathbf{P} \\
&= \frac{Kn\lambda}{K^2n\lambda + 1 - c} \left( \mathbf{I} - \frac{c}{K^2n\lambda + 1 - c + nc} \mathbf{P}^\top \mathbf{P} \right)
\end{aligned}$$

For simplicity, let us define two constants  $p$  and  $q$ :

$$p = 1 - \frac{K^2n\lambda}{K^2n\lambda + 1 - c}, \quad q = 1 - \frac{K^2n\lambda}{K^2n\lambda + 1 - c + nc}. \quad (66)$$

Then, formulate  $(\mathbf{I} - K\mathbf{B})^t$  can be formulated as

$$\begin{aligned}
(\mathbf{I} - K\mathbf{B})^t &= \left( p\mathbf{I} + \frac{1}{n}(q-p)\mathbf{P}^\top \mathbf{P} \right)^t \\
&= p^t \mathbf{I} + \sum_{i=1}^t \binom{t}{i} p^{t-i} \frac{(q-p)^i}{n^i} (\mathbf{P}^\top \mathbf{P})^i \\
&= p^t \mathbf{I} + \sum_{i=1}^t \binom{t}{i} p^{t-i} \frac{(q-p)^i}{n^i} n^{i-1} \mathbf{P}^\top \mathbf{P} \\
&= p^t \mathbf{I} + \frac{1}{n} (q^t - p^t) \mathbf{P}^\top \mathbf{P}
\end{aligned}$$

Hence, the formulation for  $\mathbf{Y}^{(t)}$  is

$$\begin{aligned}
\mathbf{Y}^{(t)} &= \left( \mathbf{Y}^{(0)} - \frac{1}{K} \mathbf{1}_{K \times Kn} \right) (\mathbf{I} - K\mathbf{B})^t + \frac{1}{K} \mathbf{1}_{K \times Kn} \\
&= \left( \mathbf{Y}^{(0)} - \frac{1}{K} \mathbf{1}_{K \times Kn} \right) \left( p^t \mathbf{I} + \frac{1}{n} (q^t - p^t) \mathbf{P}^\top \mathbf{P} \right) + \frac{1}{K} \mathbf{1}_{K \times Kn} \\
&= p^t \mathbf{Y}^{(0)} + \frac{1}{n} (q^t - p^t) \mathbf{Y}^{(0)} \mathbf{P}^\top \mathbf{P} + \frac{1}{K} (1 - q^t) \mathbf{1}_{K \times Kn}
\end{aligned}$$

Finally, we arrive at the closed form of  $\mathbf{y}_i^{(t)}$ ,

$$\mathbf{y}_i^{(t)} = p^t \mathbf{e}(\hat{y}_i) + \frac{1}{n} (q^t - p^t) \sum_{\{j: y_i = y_j\}} \mathbf{e}(\hat{y}_j) + \frac{1}{K} (1 - q^t) \mathbf{1}_K. \quad (67)$$

## E.2 Non-Constant Correlation

Let the feature correlation between the two samples with the same true label is not constant. Then, we can express feature correlation as a function of the true labels. i.e.,

$$\omega(\phi(\mathbf{x}_i), \phi(\mathbf{x}_j)) = \begin{cases} \omega(y_i), & y_i = y_j \\ 0, & y_i \neq y_j \end{cases} \quad (68)$$

Then,  $\mathbf{v}$  and  $\mathbf{W}$  can be expressed as

$$\mathbf{v} = \left[ \frac{Kn\lambda}{K^2n\lambda + 1 - \omega(i)} \right]_{i=1}^K,$$

and

$$\mathbf{W} = \mathbf{D} \left( \left[ \frac{\omega(i)}{K^2 n \lambda + 1 - \omega(i)} \right]_{i=1}^K \right).$$

As  $\mathbf{W}$  becomes a diagonal matrix, we can simplify  $\mathbf{W}^\top (\mathbf{I} + n\mathbf{W}^\top)^{-1} \mathbf{D}(\mathbf{v})$  in the following way:

$$\begin{aligned} \mathbf{W}^\top (\mathbf{I} + n\mathbf{W}^\top)^{-1} \mathbf{D}(\mathbf{v}) &= \mathbf{D} \left( \left[ \frac{\omega(i)}{K^2 n \lambda + 1 - \omega(i)} * \frac{1}{1 + \frac{n\omega(i)}{K^2 n \lambda + 1 - \omega(i)}} * \frac{Kn\lambda}{K^2 n \lambda + 1 - \omega(i)} \right]_{i=1}^K \right) \\ &= \mathbf{D} \left( \left[ \frac{Kn\lambda\omega(i)}{(K^2 n \lambda + 1 - \omega(i))(K^2 n \lambda + 1 - (n-1)\omega(i))} \right]_{i=1}^K \right) := \mathbf{D}(\mathbf{u}) \end{aligned}$$

Hence,  $\mathbf{B}$  can be formulated as follows:

$$\begin{aligned} \mathbf{B} &= \mathbf{D}(\mathbf{v}\mathbf{P}) - \mathbf{P}^\top \mathbf{W}^\top (\mathbf{I} + n\mathbf{W}^\top)^{-1} \mathbf{D}(\mathbf{v})\mathbf{P} \\ &= \mathbf{D}(\mathbf{v}\mathbf{P}) - \mathbf{P}^\top \mathbf{D}(\mathbf{u})\mathbf{P} \end{aligned}$$

Without loss of generality,  $Kn$  samples are sorted according to the order of  $y_i$ . Then,  $\mathbf{P}$  is constructed as follows:

$$\mathbf{P} = [\underbrace{\mathbf{e}_1, \dots, \mathbf{e}_1}_n, \underbrace{\mathbf{e}_2, \dots, \mathbf{e}_2}_n, \dots, \underbrace{\mathbf{e}_K, \dots, \mathbf{e}_K}_n] \quad (69)$$

Then, for any  $\mathbf{U} \in R^{K \times K}$ ,  $\mathbf{P}^\top \mathbf{U} \mathbf{P}$  can be expressed as the block matrix:

$$\mathbf{P}^\top \mathbf{U} \mathbf{P} = \begin{bmatrix} \mathbf{U}[1,1]\mathbf{1}_{n \times n} & \mathbf{U}[1,2]\mathbf{1}_{n \times n} & \cdots & \mathbf{U}[1,K]\mathbf{1}_{n \times n} \\ \mathbf{U}[2,1]\mathbf{1}_{n \times n} & \mathbf{U}[2,2]\mathbf{1}_{n \times n} & \cdots & \mathbf{U}[2,K]\mathbf{1}_{n \times n} \\ \vdots & \vdots & \ddots & \vdots \\ \mathbf{U}[K,1]\mathbf{1}_{n \times n} & \mathbf{U}[K,2]\mathbf{1}_{n \times n} & \cdots & \mathbf{U}[K,K]\mathbf{1}_{n \times n} \end{bmatrix} := [\mathbf{U}[i,j]\mathbf{1}_{n \times n}]_{i,j=1}^n$$

By (69), we have

$$\mathbf{B} = \mathbf{D}([\mathbf{v}_i \mathbf{I}]_{i=1}^K) - \mathbf{D}([\mathbf{u}_i \mathbf{1}_{n \times n}]_{i=1}^K) = \mathbf{D}([\mathbf{v}_i \mathbf{I} - \mathbf{u}_i \mathbf{1}_{n \times n}]_{i=1}^K) \quad (70)$$

Then, one can compute  $(\mathbf{I} - \mathbf{K}\mathbf{B})^t$  as follows:

$$(\mathbf{I} - \mathbf{K}\mathbf{B})^t = \mathbf{D}([(1 - K\mathbf{v}_i)\mathbf{I} + K\mathbf{u}_i \mathbf{1}_{n \times n}]_{i=1}^K)^t$$

Note that  $\mathbf{D}([A_i]_{i=1}^K)^t = \mathbf{D}([A_i^t]_{i=1}^K)$ . For each  $i$ , we have

$$\begin{aligned} ((1 - K\mathbf{v}_i)\mathbf{I} + K\mathbf{u}_i \mathbf{1}_{n \times n})^t &= (1 - K\mathbf{v}_i)^t \mathbf{I} + \sum_{j=1}^K (1 - K\mathbf{v}_i)^{t-j} (K\mathbf{u}_i)^j (\mathbf{1}_{n \times n})^j \\ &= (1 - K\mathbf{v}_i)^t \mathbf{I} + \sum_{j=1}^K (1 - K\mathbf{v}_i)^{t-j} (K\mathbf{u}_i)^j n^{j-1} \mathbf{1}_{n \times n} \\ &= (1 - K\mathbf{v}_i)^t \mathbf{I} + \frac{1}{n} ((1 - K\mathbf{v}_i + Kn\mathbf{u}_i)^t - (1 - K\mathbf{v}_i)^t) \mathbf{1}_{n \times n} \end{aligned}$$

Also,  $1 - K\mathbf{v}_i$  and  $1 - K\mathbf{v}_i + Kn\mathbf{u}_i$  can be formulated as

$$\begin{aligned} 1 - K\mathbf{v}_i &= 1 - \frac{K^2 n \lambda}{K^2 n \lambda + 1 - \omega(i)} := p_i \\ 1 - K\mathbf{v}_i + Kn\mathbf{u}_i &= 1 - \frac{K^2 n \lambda}{K^2 n \lambda + 1 - \omega(i) + n\omega(i)} := q_i \end{aligned}$$

Then,  $(\mathbf{I} - K\mathbf{B})^t$  can be represented as

$$(\mathbf{I} - K\mathbf{B})^t = \mathbf{D} \left( \left[ p_i^t \mathbf{I} + \frac{1}{n} (q_i^t - p_i^t) \mathbf{1}_{n \times n} \right]_{i=1}^K \right)$$

Please note that

$$\mathbf{1}_{K \times Kn} (\mathbf{I} - K\mathbf{B})^t[:, i] = q_{y_i}^t \mathbf{1}_K.$$

Therefore, we arrive at the closed form  $\mathbf{y}_i^{(t)}$ :

$$\begin{aligned} \mathbf{y}_i^{(t)} &= \left( \mathbf{Y}^{(0)} - \frac{1}{K} \mathbf{1}_{K \times Kn} \right) (\mathbf{I} - K\mathbf{B})^t[:, i] + \frac{1}{K} \mathbf{1}_K \\ &= \mathbf{Y}^{(0)} (\mathbf{I} - K\mathbf{B})^t[:, i] + \frac{1}{K} (1 - q_{y_i}^t) \mathbf{1}_K \\ &= p_{y_i}^t \mathbf{e}(\hat{y}_i) + \frac{1}{n} (q_{y_i}^t - p_{y_i}^t) \sum_{\{j: y_i = y_j\}} \mathbf{e}(\hat{y}_j) + \frac{1}{K} (1 - q_{y_i}^t) \mathbf{1}_K \end{aligned} \quad (71)$$

Note that the expressions for  $\mathbf{y}_i^{(t)}$  are all the same as (67) except that  $p$  and  $q$  have become  $p_{y_i}$  and  $q_{y_i}$ .

### E.3 Different Labels are Correlated (Proof of Lemma 2)

Let  $c$  be the feature correlation between two samples with the same true label, and let  $d$  be the correlation between two samples with different true labels. The equation for the correlation between two features can be defined as

$$\omega(\phi(\mathbf{x}_i), \phi(\mathbf{x}_j)) = \begin{cases} c, & y_i = y_j \\ d, & y_i \neq y_j \end{cases} \quad (72)$$

Then,  $\mathbf{I} + n\mathbf{W}^\top$  can be formulated as follows:

$$\begin{aligned} \mathbf{W} &= \frac{c - d}{K^2 n \lambda + 1 - c} \mathbf{I} + \frac{d}{K^2 n \lambda + 1 - c} \mathbf{1}_{K \times K} \\ \mathbf{I} + n\mathbf{W}^\top &= \frac{K^2 n \lambda + 1 - c + n(c - d)}{K^2 n \lambda + 1 - c} \mathbf{I} + \frac{nd}{K^2 n \lambda + 1 - c} \mathbf{1}_{K \times K} \end{aligned}$$

**Lemma 5.** (Sherman-Morrison formula) Suppose  $\mathbf{A} \in \mathbb{R}^{n \times n}$  is an invertible square matrix and  $\mathbf{u}, \mathbf{v} \in \mathbb{R}^n$  are column vectors. Then,  $\mathbf{A} + \mathbf{u}\mathbf{v}^\top$  is invertible iff  $1 + \mathbf{v}^\top \mathbf{A}^{-1} \mathbf{u} \neq 0$ . In this case,

$$(\mathbf{A} + \mathbf{u}\mathbf{v}^\top)^{-1} = \mathbf{A}^{-1} - \frac{\mathbf{A}^{-1} \mathbf{u}\mathbf{v}^\top \mathbf{A}^{-1}}{1 + \mathbf{v}^\top \mathbf{A}^{-1} \mathbf{u}} \quad (73)$$

In this case,  $\mathbf{A}$ ,  $\mathbf{u}$ , and  $\mathbf{v}$  correspond to:

$$\begin{aligned} \mathbf{A} &= \frac{K^2 n \lambda + 1 - c + n(c - d)}{K^2 n \lambda + 1 - c} \mathbf{I} \\ \mathbf{u} &= \frac{nd}{K^2 n \lambda + 1 - c} \mathbf{1}_K \\ \mathbf{v} &= \mathbf{1}_K \end{aligned}$$

Hence, we can compute  $\mathbf{W}^\top (\mathbf{I} + n\mathbf{W}^\top)^{-1} \mathbf{D}(v)$  as follows:

$$\begin{aligned} (\mathbf{I} + n\mathbf{W}^\top)^{-1} &= \frac{K^2 n \lambda + 1 - c}{K^2 n \lambda + 1 - c + n(c - d)} \mathbf{I} - \frac{\left( \frac{K^2 n \lambda + 1 - c}{K^2 n \lambda + 1 - c + n(c - d)} \right)^2 \frac{nd}{K^2 n \lambda + 1 - c}}{1 + \frac{Knd}{K^2 n \lambda + 1 - c} \frac{K^2 n \lambda + 1 - c}{K^2 n \lambda + 1 - c + n(c - d)}} \mathbf{1}_{K \times K} \\ &= \frac{K^2 n \lambda + 1 - c}{K^2 n \lambda + 1 - c + n(c - d)} \left( \mathbf{I} - \frac{nd}{K^2 n \lambda + 1 - c + n(c - d) + Knd} \mathbf{1}_{K \times K} \right) \end{aligned}$$



Define  $p$ ,  $q$ , and  $r$  according to the following equations:

$$\begin{aligned} p &= 1 - \frac{K^2 n \lambda}{K^2 n \lambda + 1 - c} \\ q &= 1 - \frac{K^2 n \lambda}{K^2 n \lambda + 1 - c + n(c - d)} \\ r &= 1 - \frac{K^2 n \lambda}{K^2 n \lambda + 1 - c + n(c - d) + K n d} \end{aligned}$$

Then, the formulation for  $(\mathbf{I} - K\mathbf{B})$  can be simplified as follows:

$$\begin{aligned} \mathbf{I} - K\mathbf{B} &= \mathbf{I} - K\mathbf{D}(v\mathbf{P}) + K\mathbf{P}^\top \mathbf{W}^\top (\mathbf{I} + n\mathbf{W}^\top)^{-1} \mathbf{D}(v)\mathbf{P} \\ &= p\mathbf{I} + \mathbf{P}^\top \left( \frac{q-p}{n} \mathbf{I} + \frac{r-q}{Kn} \mathbf{1}_{K \times K} \right) \mathbf{P} \\ &= p\mathbf{I} + \frac{q-p}{n} \mathbf{P}^\top \mathbf{P} + \frac{r-q}{Kn} \mathbf{1}_{Kn \times Kn} \end{aligned}$$

Also, by simple math, the following equations hold:

$$\begin{aligned} (\mathbf{P}^\top \mathbf{P})(\mathbf{P}^\top \mathbf{P}) &= n\mathbf{P}^\top \mathbf{P} \\ (\mathbf{P}^\top \mathbf{P})\mathbf{1}_{Kn \times Kn} &= \mathbf{1}_{Kn \times Kn}(\mathbf{P}^\top \mathbf{P}) = n\mathbf{1}_{Kn \times Kn} \\ \mathbf{1}_{Kn \times Kn}\mathbf{1}_{Kn \times Kn} &= Kn\mathbf{1}_{Kn \times Kn} \end{aligned}$$

Hence, we have

$$\begin{aligned} \left( \frac{q-p}{n} \mathbf{P}^\top \mathbf{P} + \frac{r-q}{Kn} \mathbf{1}_{Kn \times Kn} \right)^t &= \left( \frac{q-p}{n} \mathbf{P}^\top \mathbf{P} \right)^t + \sum_{i=1}^t \binom{t}{i} \left( \frac{q-p}{n} \mathbf{P}^\top \mathbf{P} \right)^{t-i} \left( \frac{r-q}{Kn} \mathbf{1}_{Kn \times Kn} \right)^i \\ &= \frac{(q-p)^t}{n} \mathbf{P}^\top \mathbf{P} + \sum_{i=1}^t \binom{t}{i} \frac{(q-p)^{t-i}}{n} \frac{(r-q)^i}{Kn} \mathbf{P}^\top \mathbf{P} \mathbf{1}_{Kn \times Kn} \\ &= \frac{(q-p)^t}{n} \mathbf{P}^\top \mathbf{P} + \frac{1}{Kn} \sum_{i=1}^t \binom{t}{i} (q-p)^{t-i} (r-q)^i \mathbf{1}_{Kn \times Kn} \\ &= \frac{(q-p)^t}{n} \mathbf{P}^\top \mathbf{P} + \frac{1}{Kn} ((r-p)^t - (q-p)^t) \mathbf{1}_{Kn \times Kn} \end{aligned}$$

Finally, we can compute  $(\mathbf{I} - K\mathbf{B})^t$  as follows:

$$\begin{aligned} (\mathbf{I} - K\mathbf{B})^t &= \left( p\mathbf{I} + \frac{q-p}{n} \mathbf{P}^\top \mathbf{P} + \frac{r-q}{Kn} \mathbf{1}_{Kn \times Kn} \right)^t \\ &= p^t \mathbf{I} + \sum_{i=1}^t \binom{t}{i} p^{t-i} \left( \frac{q-p}{n} \mathbf{P}^\top \mathbf{P} + \frac{r-q}{Kn} \mathbf{1}_{Kn \times Kn} \right)^i \\ &= p^t \mathbf{I} + \sum_{i=1}^t \binom{t}{i} p^{t-i} \left( \frac{(q-p)^i}{n} \mathbf{P}^\top \mathbf{P} + \frac{1}{Kn} ((r-p)^i - (q-p)^i) \mathbf{1}_{Kn \times Kn} \right) \\ &= p^t \mathbf{I} + \frac{1}{n} (q^t - p^t) \mathbf{P}^\top \mathbf{P} + \frac{1}{Kn} (r^t - q^t) \mathbf{1}_{Kn \times Kn} \end{aligned}$$

Now, the product  $(\mathbf{Y}^{(0)} - \frac{1}{K}\mathbf{1}_{K \times Kn})(\mathbf{I} - K\mathbf{B})^t[:, i]$  can be decomposed into three components:

$$\begin{aligned} \left(\mathbf{Y}^{(0)} - \frac{1}{K}\mathbf{1}_{K \times Kn}\right)\mathbf{I}[:, i] &= \mathbf{e}(\hat{y}_i) - \frac{1}{K}\mathbf{1}_K \\ \left(\mathbf{Y}^{(0)} - \frac{1}{K}\mathbf{1}_{K \times Kn}\right)\mathbf{P}^\top\mathbf{P}[:, i] &= \sum_{\{j:y_i=y_j\}} \mathbf{e}(\hat{y}_j) - \frac{n}{K}\mathbf{1}_K \\ \left(\mathbf{Y}^{(0)} - \frac{1}{K}\mathbf{1}_{K \times Kn}\right)\mathbf{1}_{Kn} &= \sum_{j=1}^{Kn} \mathbf{e}(\hat{y}_j) - n\mathbf{1}_K \end{aligned}$$

Finally, we obtain the closed form for  $\mathbf{y}_i^{(t)}$ :

$$\begin{aligned} \mathbf{y}_i^{(t)} &= \left(\mathbf{Y}^{(0)} - \frac{1}{K}\mathbf{1}_{K \times Kn}\right)(\mathbf{I} - K\mathbf{B})^t[:, i] + \frac{1}{K}\mathbf{1}_K \\ &= p^t\mathbf{e}(\hat{y}_i) + (q^t - p^t)\left(\frac{1}{n}\sum_{\{j:y_i=y_j\}} \mathbf{e}(\hat{y}_j)\right) + (r^t - q^t)\left(\frac{1}{Kn}\sum_{j=1}^{Kn} \mathbf{e}(\hat{y}_j)\right) + (1 - r^t)\frac{1}{K}\mathbf{1}_K \\ &= p^t\mathbf{e}(\hat{y}_i) + (q^t - p^t)\left(\frac{1}{n}\sum_{\{j:y_i=y_j\}} \mathbf{e}(\hat{y}_j)\right) + (1 - q^t)\frac{1}{K}\mathbf{1}_K \end{aligned} \quad (74)$$

The last equality holds because of the balance of the provided label,  $\{\hat{y}_i\}$ . Please note that the closed form for  $\mathbf{y}_i^{(t)}$  consists of the following three components, across all three scenarios:

- $\mathbf{e}(\hat{y}_i)$ : the provided label,
- $\frac{1}{n}\sum_{\{j:y_i=y_j\}} \mathbf{e}(\hat{y}_j)$ : the mean of the provided labels for samples that share the same true label, and
- $\frac{1}{K}\mathbf{1}_K$ : the uniform vector.

## F Label Noise

In this section, we will discuss about the label noise. We define the corruption matrix  $\mathbf{C} \in \mathbb{R}^{K \times K}$  as

$$[\mathbf{C}]_{k,k'} := \frac{|\{i : y_i = k, \hat{y}_i = k'\}|}{n}.$$

Then, the mean of the provided labels for samples that share the same true label, denoted as  $\frac{1}{n}\sum_{\{j:y_i=y_j\}} \mathbf{e}(\hat{y}_j)$ , corresponds to the  $y_i$ -th column of the matrix  $\mathbf{C}$ , expressed as:

$$\frac{1}{n}\sum_{\{j:y_i=y_j\}} \mathbf{e}(\hat{y}_j) = [\mathbf{C}_{y_i, \cdot}]^\top.$$

Here, we aim to find the conditions for the prediction vector  $\mathbf{y}_i^{(t)}$  has the maximum value at the true label  $y_i$ , indicating a correct prediction. To achieve this, we will use the closed-form solution from Lemma 2.

### F.1 The $t$ -th Distilled Model

According to Lemma 2, the closed-form outputs of the  $t$ -th distilled model can be formulated as

$$\mathbf{y}_i^{(t)} = p^t\mathbf{e}(\hat{y}_i) + (q^t - p^t)\left(\frac{1}{n}\sum_{\{j:y_i=y_j\}} \mathbf{e}(\hat{y}_j)\right) + \frac{(1 - q^t)}{K}\mathbf{1}_K,$$

where  $p$  and  $q$  are defined as in (19).

For the clean sample, i.e.,  $\hat{y}_i = y_i$ , the prediction of the  $t$ -th distilled model for the  $i$ -th sample can be written as

$$[\mathbf{y}_i^{(t)}]_j = \begin{cases} p^t + (q^t - p^t)[\mathbf{C}]_{y_i, y_i} + (1 - q)/K, & j = y_i \\ (q^t - p^t)[\mathbf{C}]_{y_i, j} + (1 - q)/K. & j \neq y_i \end{cases}$$

Then, the condition for the correct classification of the clean sample  $i$  is given by

$$[\mathbf{C}]_{y_i, y_i} > [\mathbf{C}]_{y_i, k} - \frac{1}{(q/p)^t - 1}, \quad \forall k \neq y_i \quad (75)$$

For the noisy sample, the prediction of the  $t$ -th distilled model can be written as

$$[\mathbf{y}_i^{(t)}]_j = \begin{cases} (q^t - p^t)[\mathbf{C}]_{y_i, y_i} + (1 - q)/K, & j = y_i \\ p^t + (q^t - p^t)[\mathbf{C}]_{y_i, \hat{y}_i} + (1 - q)/K, & j = \hat{y}_i \\ (q^t - p^t)[\mathbf{C}]_{y_i, j} + (1 - q)/K, & j \neq y_i, \hat{y}_i \end{cases}$$

The condition for the correct classification of the noisy sample  $i$  is given as

$$[\mathbf{C}]_{y_i, y_i} > [\mathbf{C}]_{y_i, \hat{y}_i} + \frac{1}{(q/p)^t - 1} \quad (76)$$

$$[\mathbf{C}]_{y_i, y_i} > [\mathbf{C}]_{y_i, k}, \quad \forall k \neq y_i, \hat{y}_i \quad (77)$$

Note that (75) is the easiest condition, and (76) is the hardest condition. To find the regimes where the student model outperforms the teacher model, we need to find  $t$  that satisfies the following:

$$[\mathbf{C}]_{y_i, \hat{y}_i} + \frac{1}{(q/p)^{t-1} - 1} > [\mathbf{C}]_{y_i, y_i} > [\mathbf{C}]_{y_i, \hat{y}_i} + \frac{1}{(q/p)^t - 1}, \quad (78)$$

In such  $t$ , the student model correctly classifies the samples whose true labels are  $y_i$  and the provided label are  $\hat{y}_i$ , but teacher model makes mistakes.

## F.2 PLL Student Model

Recall the closed form of the PLL student model from Lemma 2:

$$\mathbf{y}_i^{(P)} = p\bar{\mathbf{y}}_i + \frac{1}{n}(q - p) \sum_{\{j: y_i = y_j\}} \bar{\mathbf{y}}_j + \frac{1}{K}(1 - q)\mathbf{1}_K. \quad (79)$$

Note that  $\bar{\mathbf{y}}$  represents the two-hot vectors composed of the two labels with the highest values in the teacher's predictions.

Suppose  $[\mathbf{C}]_{y_i, y_i} > [\mathbf{C}]_{y_i, k}$  holds for all  $k \neq y_i$ . From condition (75) and (77), true label is always included the candidate set of PLL. Let us define  $\tilde{y}_i$  as

$$\tilde{y}_i = \arg \max_{k \neq y_i} [\mathbf{C}]_{y_i, k}. \quad (80)$$

Then, the equation for  $\bar{\mathbf{y}}_i$  can be expressed as:

$$\bar{\mathbf{y}}_i = \frac{1}{2}\mathbf{e}(y_i) + \frac{1}{2}\mathbf{e}(\tilde{y}_i) \quad (81)$$

for the clean sample, and

$$\bar{\mathbf{y}}_i = \frac{1}{2}\mathbf{e}(y_i) + \frac{1}{2}\mathbf{e}(\hat{y}_i) \quad (82)$$

for the noisy sample. Then,  $\frac{1}{n} \sum_{\{j:y_i=y_j\}} \bar{y}_j$  is given as

$$\frac{1}{n} \sum_{\{j:y_i=y_j\}} \bar{y}_j = \frac{1}{2} \mathbf{e}(y_i) + \frac{1}{2} [\mathbf{C}]_{y_i, y_i} \mathbf{e}(\tilde{y}_i) + \frac{1}{2} \sum_{j \neq y_i} [\mathbf{C}]_{y_i, j} \mathbf{e}(j). \quad (83)$$

For the clean sample, the prediction of the PLL student model for the  $i$ -th sample can be written as

$$[\mathbf{y}_i^{(P)}]_j = \begin{cases} \frac{p}{2} + \frac{q-p}{2} + (1-q)/K, & j = y_i \\ \frac{p}{2} + \frac{q-p}{2} ([\mathbf{C}]_{y_i, y_i} + [\mathbf{C}]_{y_i, \tilde{y}_i}) + (1-q)/K, & j = \tilde{y}_i \\ \frac{q-p}{2} [\mathbf{C}]_{y_i, j} e(j) + (1-q)/K, & j \neq y_i, \tilde{y}_i \end{cases}$$

Here,  $\mathbf{y}_i^{(P)}$  has the maximum value at  $j = y_i$ , because  $[\mathbf{C}]_{y_i, y_i} + [\mathbf{C}]_{y_i, \tilde{y}_i}$  is less than or equal to 1. For the noisy sample, when  $\hat{y}_i = \tilde{y}_i$ , we have

$$[\mathbf{y}_i^{(t)}]_j = \begin{cases} \frac{p}{2} + \frac{q-p}{2} + (1-q)/K, & j = y_i \\ \frac{p}{2} + \frac{q-p}{2} ([\mathbf{C}]_{y_i, y_i} + [\mathbf{C}]_{y_i, \tilde{y}_i}) + (1-q)/K, & j = \hat{y}_i \\ \frac{q-p}{2} [\mathbf{C}]_{y_i, j} e_j + (1-q)/K, & j \neq y_i, \hat{y}_i \end{cases}$$

On the other hand, when  $\hat{y}_i \neq \tilde{y}_i$ , we have

$$[\mathbf{y}_i^{(t)}]_j = \begin{cases} \frac{p}{2} + \frac{q-p}{2} + (1-q)/K, & j = y_i \\ \frac{p}{2} + \frac{q-p}{2} [\mathbf{C}]_{y_i, \hat{y}_i} + (1-q)/K, & j = \hat{y}_i \\ \frac{q-p}{2} ([\mathbf{C}]_{y_i, y_i} + [\mathbf{C}]_{y_i, \tilde{y}_i}) + (1-q)/K, & j = \tilde{y}_i \\ \frac{q-p}{2} [\mathbf{C}]_{y_i, j} e_j + (1-q)/K, & j \neq y_i, \hat{y}_i, \tilde{y}_i \end{cases}$$

Therefore, the prediction of the PLL student model has the highest probability at the true label  $y_i$  for all noisy samples.

Throughout all cases, it can be concluded that the PLL model consistently achieves 100% population accuracy when candidate sets always contain the true label. Please note that the condition for this situation is given in (77).

To summarize, the  $t$ -th distilled model attains 100% population accuracy when

$$[\mathbf{C}]_{y_i, y_i} > [\mathbf{C}]_{y_i, \tilde{y}_i} + \frac{1}{(q/p)^t - 1}$$

holds. For the PLL student model, the condition for achieving 100% population accuracy is given by

$$[\mathbf{C}]_{y_i, y_i} > [\mathbf{C}]_{y_i, \tilde{y}_i},$$

which implies that the PLL student model outperforms any  $t$ -th distilled model in the population accuracy.

## G More Empirical Results

We perform an ablation study for  $\lambda$  values that resulted in  $q/p$  near 2 as explained in Sec. B.3. For these  $\lambda$  values, we observe that there is a consistent accuracy gain as the distillation round  $t$  increases.

Table 3: ResNet18 training with CIFAR-10 datasets, where weight decay value is  $\lambda = 1 \times 10^{-6}$ .

	Symmetric				Asymmetric			
	0.7	0.75	0.8	0.85	0.7	0.75	0.8	0.85
$t = 1$	67.75±0.36%	60.58±0.27%	49.22±0.29%	32.03±1.99%	65.36±0.12%	55.89±0.96%	42.44±1.42%	25.70±1.37%
$t = 2$	70.22±0.45%	64.02±0.45%	53.08±1.86%	31.17±1.09%	<b>66.44±0.90%</b>	57.82±1.45%	43.06±1.78%	22.79±0.42%
$t = 3$	70.21±0.20%	64.29±0.12%	53.55±0.96%	31.72±1.32%	66.26±1.04%	57.58±1.72%	43.50±1.23%	23.06±0.55%
$t = 4$	<b>70.71±0.12%</b>	64.40±0.37%	53.25±1.33%	31.84±1.33%	66.39±0.73%	<b>57.93±1.85%</b>	43.28±1.16%	23.16±0.60%
PLL	68.78±0.55%	<b>64.89±0.83%</b>	<b>59.40±2.25%</b>	<b>37.06±1.57%</b>	62.06±0.36%	56.84±1.96%	<b>45.94±2.52%</b>	<b>25.72±0.75%</b>

Table 4: ResNet18 training with CIFAR-10 datasets, where weight decay value is  $\lambda = 5 \times 10^{-7}$ .

	Symmetric				Asymmetric			
	0.7	0.75	0.8	0.85	0.7	0.75	0.8	0.85
$t = 1$	67.87±0.32%	60.55±0.75%	49.04±1.25%	31.54±0.22%	65.84±1.89%	56.64±0.54%	42.94±1.01%	25.01±0.74%
$t = 2$	70.54±1.04%	64.29±0.31%	53.19±0.80%	34.07±0.32%	67.79±0.88%	59.45±0.32%	45.01±0.63%	23.86±1.08%
$t = 3$	<b>70.72±1.13%</b>	64.18±0.38%	52.63±0.05%	33.50±0.41%	68.22±0.98%	59.49±0.61%	44.47±0.52%	23.53±1.05%
$t = 4$	70.69±1.14%	64.12±0.20%	52.45±0.37%	34.04±0.89%	<b>68.35±1.00%</b>	<b>59.62±0.41%</b>	45.13±0.81%	23.69±1.74%
PLL	69.56±0.27%	<b>65.31±0.95%</b>	<b>57.92±0.73%</b>	<b>41.68±2.46%</b>	63.18±0.12%	58.03±1.19%	<b>47.49±1.34%</b>	<b>26.51±1.42%</b>

Table 5: ResNet34 training with CIFAR-100 datasets, where weight decay value is  $\lambda = 1 \times 10^{-7}$ .

	Symmetric				Asymmetric			
	0.7	0.75	0.8	0.85	0.7	0.75	0.8	0.85
$t = 1$	51.56±0.24%	47.54±0.05%	43.26±0.45%	35.79±0.39%	50.93±0.57%	47.08±0.53%	42.74±0.56%	35.28±0.32%
$t = 2$	53.17±0.28%	49.64±0.32%	45.30±0.06%	37.99±0.43%	52.81±0.36%	49.54±0.61%	45.48±0.41%	37.97±0.48%
$t = 3$	53.28±0.22%	<b>49.96±0.32%</b>	45.32±0.27%	38.48±0.22%	<b>53.10±0.17%</b>	49.97±0.62%	45.62±0.49%	38.19±0.14%
$t = 4$	<b>53.32±0.37%</b>	49.85±0.38%	45.25±0.16%	38.67±0.15%	53.04±0.27%	49.81±0.75%	45.85±0.34%	38.28±0.49%
PLL	52.38±0.12%	49.92±0.35%	<b>46.85±0.04%</b>	<b>42.17±0.10%</b>	52.36±0.21%	<b>50.28±0.41%</b>	<b>47.67±0.34%</b>	<b>42.12±0.36%</b>

Table 6: ResNet34 training with CIFAR-100 datasets, where weight decay value is  $\lambda = 5 \times 10^{-7}$ .

	Symmetric				Asymmetric			
	0.7	0.75	0.8	0.85	0.7	0.75	0.8	0.85
$t = 1$	50.86±0.09%	47.41±0.20%	42.65±0.21%	35.07±0.25%	51.11±0.28%	47.52±0.36%	42.97±0.90%	35.20±0.46%
$t = 2$	52.67±0.12%	49.49±0.21%	45.14±0.11%	37.46±0.32%	52.44±0.41%	49.61±0.09%	45.23±0.56%	37.68±0.53%
$t = 3$	52.76±0.23%	49.81±0.24%	45.07±0.13%	37.62±0.10%	<b>52.71±0.41%</b>	49.86±0.38%	45.39±0.46%	38.06±0.52%
$t = 4$	<b>52.88±0.11%</b>	49.71±0.08%	45.36±0.18%	37.81±0.13%	52.65±0.55%	49.91±0.14%	45.35±0.20%	38.40±0.22%
PLL	52.00±0.02%	<b>50.09±0.16%</b>	<b>47.02±0.39%</b>	<b>42.08±0.24%</b>	52.26±0.04%	<b>50.11±0.43%</b>	<b>47.18±0.44%</b>	<b>41.87±0.38%</b>